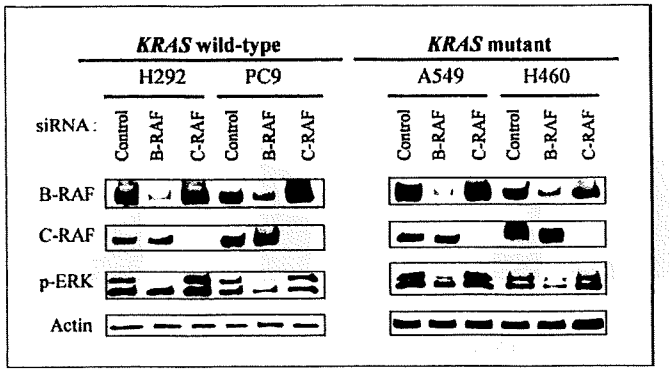

Figure 4. Effects of transient depletion of B-RAF or C-RAF on ERK phosphorylation in NSCLC cells. Cells harboring wild-type or mutant *KRAS* were transfected with nonspecific (control), B-RAF, or C-RAF siRNAs for 48 h, after which cell lysates were prepared and subjected to immunoblot analysis with antibodies to B-RAF, C-RAF, phosphorylated ERK, and β-actin (loading control).

that transfection of NSCLC cells with siRNAs specific for B-RAF or C-RAF mRNAs resulted in marked and selective depletion of the corresponding protein (Fig. 4). Such depletion of B-RAF resulted in inhibition of ERK phosphorylation in cells harboring wild-type or mutant *KRAS*, whereas depletion of C-RAF had no such effect (Fig. 4). These data thus suggested that depletion of B-RAF, but not that of C-RAF, inhibits ERK phosphorylation regardless of *KRAS* status.

Effects of RAF depletion on NSCLC cell proliferation. We next examined the effects of B-RAF or C-RAF depletion on NSCLC cell proliferation and cell cycle distribution. Depletion of B-RAF resulted in significant inhibition of cell proliferation (Fig. 5*A*) and an increase in the proportion of cells in G_1 phase of the cell cycle (Fig. 5*B*), whereas depletion of C-RAF had no such effects, in NSCLC cells harboring wild-type *KRAS*. In contrast, depletion of C-RAF induced significant inhibition of cell proliferation (Fig. 5*A*) and an increase in the proportion of cells in G_1 phase (Fig. 5*B*), whereas depletion of B-RAF had only a less pronounced effect on cell proliferation, in NSCLC cells with mutant *KRAS*. These data thus suggested that B-RAF-ERK signaling regulates cell proliferation in NSCLC cells with wild-type *KRAS*, whereas C-RAF signaling mediates such regulation in NSCLC cells with mutant *KRAS*.

Sorafenib or C-RAF depletion inhibits cyclin E expression in NSCLC cells with mutant *KRAS*. Finally, to characterize further the growth inhibition and G_1 arrest induced by C-RAF depletion or sorafenib in NSCLC cells with mutant *KRAS*, we examined the expression of cyclin E, an essential promoter of the transition from G_1 to S phase of the cell cycle (19). Immunoblot analysis revealed that depletion of C-RAF in A549 or H460 cells resulted in pronounced inhibition of cyclin E expression, whereas depletion of B-RAF had no such effect (Fig. 6). Exposure of the cells to sorafenib also induced loss of cyclin E (Fig. 6). These results thus suggest that the G_1 arrest induced by depletion of C-RAF or by sorafenib in NSCLC cells with mutant *KRAS* may be attributable to the down-regulation of cyclin E.

Discussion

RAS is an upstream component of the ERK signaling pathway, which is aberrantly activated by oncogenic mutations of RAS genes. Among RAS family genes, mutations of *KRAS* are most common in solid malignancies, including NSCLC (8, 20, 21). Indeed, *KRAS* mutations have been associated with poor prognosis and resistance to conventional cytotoxic chemotherapy in NSCLC (22–24). Whereas EGFR tyrosine kinase inhibitors are most efficacious in NSCLC patients with *EGFR* mutations, *KRAS* mutations are associated with resistance to these agents (25–28). The development of therapeutic strategies for NSCLC patients with *KRAS* mutations is thus an important clinical goal. RAF serine-threonine kinases are the principal effectors of RAS in the ERK signaling pathway. Given the key role of this pathway in tumor growth, RAF is a potential target for cancer therapy.

Sorafenib is an orally available compound that has been developed as a multikinase inhibitor with activity against RAF and several RTKs. The sensitivity of cancer cells to sorafenib might be expected to be affected by *KRAS* status, given that *KRAS* mutations result in activation of the ERK pathway (8). However, as far as we are aware, no previous study has compared sorafenib sensitivity among a panel of tumor cell lines of different *KRAS* mutational status. We have now evaluated the effects of sorafenib on the growth of NSCLC cells harboring wild-type or mutant forms of *KRAS* with two different assay systems, the MTT assay and anchorage-independent colony formation assay, given that previous studies have revealed differences in the sensitivity of cells to tested drugs between these two assay systems (29). The IC_{50} values for inhibition of cell growth by sorafenib in these assays have generally been found to be well below 15 μmol/L, the maximum achievable plasma concentration of this drug (17). We found that the potency of sorafenib for inhibition of cell growth was similar for NSCLC cells regardless of *KRAS* mutational status in both assay systems. We also performed a longer-term clonogenic survival assay and again found that sorafenib inhibited the survival of NSCLC cells regardless of *KRAS* status (data not shown). These results thus indicate that sorafenib inhibits the growth of NSCLC cells with mutant *KRAS* as well as it does that of those with wild-type *KRAS* in a clinically relevant concentration range.

We have shown that sorafenib inhibited ERK phosphorylation and induced G_1 arrest in NSCLC cells with wild-type *KRAS*, consistent with previous results obtained with several cancer cell lines harboring wild-type *KRAS* (13, 30, 31). Inhibition of the ERK signaling pathway, as reflected by a reduced level of ERK phosphorylation, results in inhibition of cell proliferation and induction of G_1 arrest in various cell types (32–35). In the present study, we found that depletion of B-RAF by RNA interference also inhibited ERK phosphorylation as well as attenuated cell proliferation and induced G_1 arrest in NSCLC cells with wild-type *KRAS*. These results suggest that inhibition of B-RAF-ERK signaling contributes to suppression of the growth of NSCLC cells harboring wild-type *KRAS* by sorafenib. Consistent with these findings, the specific B-RAF inhibitor SB-590885 was previously shown to inhibit ERK phosphorylation and to induce G_1 arrest in melanoma cells with wild-type *KRAS* (36, 37). In contrast, we found that depletion of C-RAF did not result in inhibition of ERK phosphorylation in NSCLC cells. ERK activation was previously shown to be conserved in cells derived from C-RAF knockout mice, suggesting that C-RAF is dispensable for ERK signaling (38, 39). Together, the present data suggest that B-RAF-ERK signaling, rather than C-RAF signaling, is a potential therapeutic target in NSCLC cells with wild-type *KRAS*.

We showed that ERK phosphorylation was not inhibited by sorafenib in two NSCLC cell lines (A549 and H460) harboring mutant *KRAS*, consistent with previous observations (16). We further showed this to be the case in two additional such cell lines (H358 and H23). Such results were previously suggested to be due to the existence of RAF-independent ERK activation in

NSCLC cells with mutant *KRAS* (16). However, we have now shown that B-RAF depletion resulted in inhibition of ERK activation in these cells. Our data therefore suggest that sorafenib is not able to attenuate the constitutive activation of the B-RAF-ERK pathway characteristic of NSCLC cells harboring mutant *KRAS* (40). Despite the sustained activation of B-RAF-ERK signaling in such cells, sorafenib inhibited cell proliferation and induced G_1 arrest in NSCLC cells with mutant *KRAS* as well as in those with wild-type *KRAS*. These data suggest that sorafenib targets a different pathway in its inhibitory effect on cell growth in NSCLC cells with mutant *KRAS*. Whereas sorafenib inhibits the kinase activity of both B-RAF and C-RAF, it shows a higher affinity for C-RAF (16). We found that depletion of C-RAF by RNA interference inhibited cell proliferation and induced G_1 arrest, without affecting ERK phosphorylation, in NSCLC cells with mutant *KRAS*, whereas it did not exhibit such effects in NSCLC cells harboring wild-type *KRAS*. Depletion of B-RAF also inhibited the growth of NSCLC cells with mutant *KRAS*, although this effect was not as pronounced as that in those with wild-type *KRAS*. These data indicate that NSCLC cells with mutant *KRAS* are dependent on C-RAF signaling to a greater extent than on B-RAF-ERK signaling for cell proliferation but that both pathways participate in regulation of the growth of these cells. Melanoma cells that have acquired resistance to a specific B-RAF inhibitor were recently shown to have switched their dependency from B-RAF to C-RAF (41). These observations suggest that RAF proteins are functionally interchangeable in the regulation of cell growth. Our data thus indicate that C-RAF signaling is a potential therapeutic target in NSCLC cells with mutant *KRAS*. RAF family proteins are also implicated in regulation of cell cycle progression in a manner independent of the ERK pathway (18, 38, 42, 43). C-RAF has been shown to exist in a complex with Cdc25, which activates the cyclin E-Cdk2 complex and promotes the G_1-S phase transition (44, 45). Cyclin E is thus postulated to be a downstream effector of C-RAF. In the present study, we found that either C-RAF depletion or sorafenib treatment induced G_1 arrest and down-regulation of cyclin E in NSCLC cells with mutant *KRAS*. Although we cannot exclude a possible role for other cell cycle

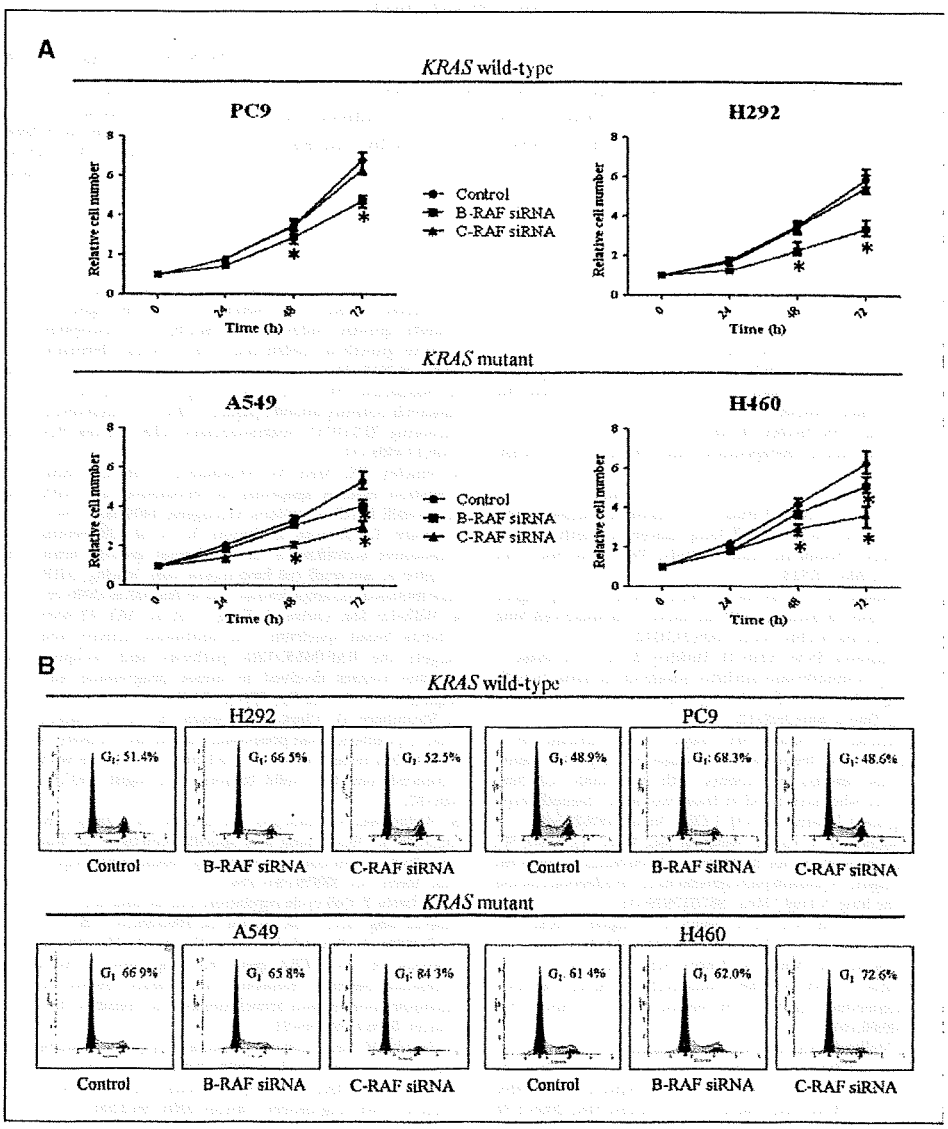

Figure 5. Effects of B-RAF or C-RAF depletion on cell proliferation and cell cycle distribution in NSCLC cells. *A*, cells harboring wild-type or mutant *KRAS* were transfected with nonspecific (control), B-RAF, or C-RAF siRNAs for the indicated times, after which the number of viable cells was determined by staining with trypan blue. The number of viable cells is expressed relative to the value for time 0. *Points*, mean values from three independent experiments; *bars*, SD. *, $P < 0.05$ versus the corresponding value for cells transfected with the nonspecific siRNA. *B*, cells were transfected as in *A* for 48 h, fixed, stained with propidium iodide, and analyzed for cell cycle distribution by flow cytometry. The percentage of cells in G_1 phase is indicated. Data are from representative experiments that were repeated on three separate occasions.

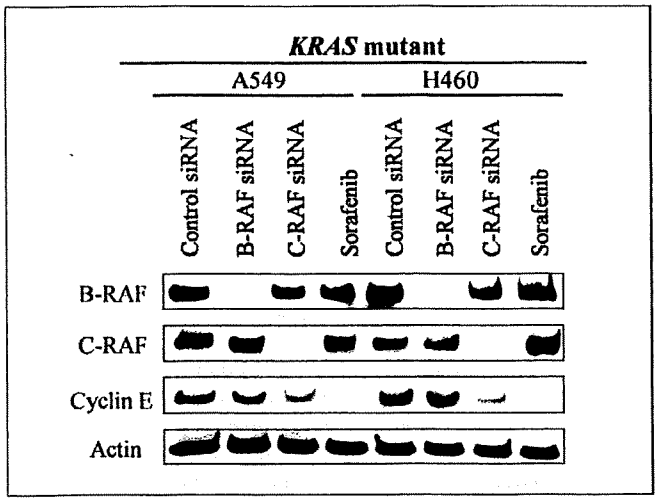

Figure 6. Effects of C-RAF depletion or sorafenib on cyclin E expression in NSCLC cells with mutant *KRAS*. Cells harboring mutant *KRAS* were transiently transfected for 48 h with nonspecific (control), B-RAF, or C-RAF siRNAs or were exposed to 15 μmol/L sorafenib for 24 h in complete medium. Cell lysates were then prepared and subjected to immunoblot analysis with antibodies to B-RAF, C-RAF, cyclin E, and β-actin.

proteins, our present data suggest that the observed down-regulation of cyclin E may contribute to the G_1 arrest induced by C-RAF depletion or by sorafenib in NSCLC cells with mutant *KRAS*.

Sorafenib inhibits several RTKs that participate in neovascularization, including vascular endothelial growth factor receptor (VEGFR)-2 and VEGFR-3 (16). Inhibition of angiogenesis might thus be expected to contribute to the inhibition of tumor growth by this drug in addition to its effects on RAF signaling. Although sorafenib was previously shown to inhibit the growth of a variety of human tumor xenografts in mice (13, 16, 46), it has been difficult to measure the relative contributions of its antiangiogenic activity and its direct antitumor activity mediated by RAF inhibition. In the present study, we have provided insight into the inhibitory effect of sorafenib on tumor cell growth *in vitro* that is mediated by inhibition of RAF signaling pathways. Our results suggest that sorafenib targets B-RAF in NSCLC cells with wild-type *KRAS* and C-RAF in those with mutant *KRAS*, and they provide a rationale for future clinical investigation of the therapeutic efficacy of sorafenib for NSCLC patients.

Disclosure of Potential Conflicts of Interest

No potential conflicts of interest were disclosed.

Acknowledgments

Received 3/23/09; revised 5/22/09; accepted 6/15/09; published OnlineFirst 7/28/09.

The costs of publication of this article were defrayed in part by the payment of page charges. This article must therefore be hereby marked *advertisement* in accordance with 18 U.S.C. Section 1734 solely to indicate this fact.

We thank H. Saya, K. Nishio, and T. Arao for helpful discussion.

References

1. Jemal A, Siegel R, Ward E, et al. Cancer statistics, 2008. CA Cancer J Clin 2008;58:71–96.
2. Eccles SA. Parallels in invasion and angiogenesis provide pivotal points for therapeutic intervention. Int J Dev Biol 2004;48:583–98.
3. Sridhar SS, Hedley D, Siu LL. Raf kinase as a target for anticancer therapeutics. Mol Cancer Ther 2005;4:677–85.
4. Adjei AA, Hillman SL. A front-line window of opportunity phase II study of sorafenib in patients with advanced non-small cell lung cancer: a North Central Cancer Treatment Group Study. Proc Am Soc Clin Oncol 2007;25:S18.
5. Gatzemeier U, Fosella F. Phase II trial of singe-agent sorafenib in patients with advanced non-small cell lung carcinoma. J Clin Oncol 2006;24:7002.
6. Gutierrez SKM, Allen D, Turkbey B, et al. A phase II study of multikinase inhibitor sorafenib in patients with relapsed non-small cell lung cancer [abstract 19084]. J Clin Oncol 2008;26:S712.
7. Schiller JH, Hanna NH, Traynor AM, Carbone DP. A randomized discontinuation phase II study of sorafenib versus placebo in patients with non-small cell lung cancer who have failed at least two prior chemotherapy regimens [abstract 8014]. J Clin Oncol 2008;26:S427.
8. Rodenhuis S, van de Wetering ML, Mooi WJ, Evers SG, van Zandwijk N, Bos JL. Mutational activation of the K-ras oncogene. A possible pathogenetic factor in adenocarcinoma of the lung. N Engl J Med 1987;317:929–35.
9. Garnett MJ, Marais R. Guilty as charged: B-RAF is a human oncogene. Cancer Cell 2004;6:313–9.
10. Panka DJ, Wang W, Atkins MB, Mier JW. The Raf inhibitor BAY 43-9006 (sorafenib) induces caspase-independent apoptosis in melanoma cells. Cancer Res 2006;66:1611–9.
11. Molhoek KR, Brautigan DL, Slingluff CL, Jr. Synergistic inhibition of human melanoma proliferation by combination treatment with B-Raf inhibitor BAY43-9006 and mTOR inhibitor rapamycin. J Transl Med 2005;3:39.
12. Lasithiotakis KG, Sinnberg TW, Schittek B, et al. Combined inhibition of MAPK and mTOR signaling inhibits growth, induces cell death, and abrogates invasive growth of melanoma cells. J Invest Dermatol 2008;128:2013–23.
13. Henderson YC, Ahn SH, Kang Y, Clayman GL. Sorafenib potently inhibits papillary thyroid carcinomas harboring RET/PTC1 rearrangement. Clin Cancer Res 2008;14:4908–14.
14. Smalley KS, Xiao M, Villanueva J, et al. CRAF inhibition induces apoptosis in melanoma cells with non-V600E BRAF mutations. Oncogene 2009;28:85–94.
15. Okabe T, Okamoto I, Tamura K, et al. Differential constitutive activation of the epidermal growth factor receptor in non-small cell lung cancer cells bearing EGFR gene mutation and amplification. Cancer Res 2007;67:2046–53.
16. Wilhelm SM, Carter C, Tang L, et al. BAY 43-9006 exhibits broad spectrum oral antitumor activity and targets the RAF/MEK/ERK pathway and receptor tyrosine kinases involved in tumor progression and angiogenesis. Cancer Res 2004;64:7099–109.
17. Strumberg D, Clark JW, Awada A, et al. Safety, pharmacokinetics, and preliminary antitumor activity of sorafenib: a review of four phase I trials in patients with advanced refractory solid tumors. Oncologist 2007;12:426–37.
18. Wojnowski L, Stancato LF, Larner AC, Rapp UR, Zimmer A. Overlapping and specific functions of Braf and Craf-1 proto-oncogenes during mouse embryogenesis. Mech Dev 2000;91:97–104.
19. Dobashi Y. Cell cycle regulation and its aberrations in human lung carcinoma. Pathol Int 2005;55:95–105.
20. Buttitta F, Barassi F, Fresu G, et al. Mutational analysis of the HER2 gene in lung tumors from Caucasian patients: mutations are mainly present in adenocarcinomas with bronchioloalveolar features. Int J Cancer 2006;119:2586–91.
21. Suzuki M, Shigematsu H, Iizasa T, et al. Exclusive mutation in epidermal growth factor receptor gene, HER-2, and KRAS, and synchronous methylation of nonsmall cell lung cancer. Cancer 2006;106:2200–7.
22. Graziano SL, Gamble GP, Newman NB, et al. Prognostic significance of K-ras codon 12 mutations in patients with resected stage I and II non-small-cell lung cancer. J Clin Oncol 1999;17:668–75.
23. Slebos RJ, Kibbelaar RE, Dalesio O, et al. K-ras oncogene activation as a prognostic marker in adenocarcinoma of the lung. N Engl J Med 1990;323:561–5.
24. Winton T, Livingston R, Johnson D, et al. Vinorelbine plus cisplatin vs. observation in resected non-small-cell lung cancer. N Engl J Med 2005;352:2589–97.
25. Pao W, Wang TY, Riely GJ, et al. KRAS mutations and primary resistance of lung adenocarcinomas to gefitinib or erlotinib. PLoS Med 2005;2:e17.
26. Massarelli E, Varella-Garcia M, Tang X, et al. KRAS mutation is an important predictor of resistance to therapy with epidermal growth factor receptor tyrosine kinase inhibitors in non-small-cell lung cancer. Clin Cancer Res 2007;13:2890–6.
27. Marks JL, Broderick S, Zhou Q, et al. Prognostic and therapeutic implications of EGFR and KRAS mutations in resected lung adenocarcinoma. J Thorac Oncol 2008;3:111–6.
28. Baselga J, Rosen N. Determinants of RASistance to anti-epidermal growth factor receptor agents. J Clin Oncol 2008;26:1582–4.
29. Hao H, Muniz-Medina VM, Mehta H, et al. Context-dependent roles of mutant B-Raf signaling in melanoma and colorectal carcinoma cell growth. Mol Cancer Ther 2007;6:2220–9.
30. Jane EP, Premkumar DR, Pollack IF. Coadministration of sorafenib with rottlerin potently inhibits cell proliferation and migration in human malignant glioma cells. J Pharmacol Exp Ther 2006;319:1070–80.
31. Ambrosini G, Cheema HS, Seelman S, et al. Sorafenib inhibits growth and mitogen-activated protein kinase signaling in malignant peripheral nerve sheath cells. Mol Cancer Ther 2008;7:890–6.
32. Villanueva J, Yung Y, Walker JL, Assoian RK. ERK activity and G_1 phase progression: identifying dispensable versus essential activities and primary versus secondary targets. Mol Biol Cell 2007;18:1457–63.

33. Jones SM, Kazlauskas A. Growth-factor-dependent mitogenesis requires two distinct phases of signalling. Nat Cell Biol 2001;3:165–72.
34. Yamamoto T, Ebisuya M, Ashida F, Okamoto K, Yonehara S, Nishida E. Continuous ERK activation downregulates antiproliferative genes throughout G_1 phase to allow cell-cycle progression. Curr Biol 2006;16:1171–82.
35. Fassett JT, Tobolt D, Nelsen CJ, Albrecht JH, Hansen LK. The role of collagen structure in mitogen stimulation of ERK, cyclin D1 expression, and G_1-S progression in rat hepatocytes. J Biol Chem 2003;278:31691–700.
36. Smalley KS, Lioni M, Dalla Palma M, et al. Increased cyclin D1 expression can mediate BRAF inhibitor resistance in BRAF V600E-mutated melanomas. Mol Cancer Ther 2008;7:2876–83.
37. King AJ, Patrick DR, Batorsky RS, et al. Demonstration of a genetic therapeutic index for tumors expressing oncogenic BRAF by the kinase inhibitor SB-590885. Cancer Res 2006;66:11100–5.
38. Huser M, Luckett J, Chiloeches A, et al. MEK kinase activity is not necessary for Raf-1 function. EMBO J 2001;20:1940–51.
39. Mikula M, Schreiber M, Husak Z, et al. Embryonic lethality and fetal liver apoptosis in mice lacking the c-raf-1 gene. EMBO J 2001;20:1952–62.
40. Salgia R, Skarin AT. Molecular abnormalities in lung cancer. J Clin Oncol 1998;16:1207–17.
41. Montagut C, Sharma SV, Shioda T, et al. Elevated CRAF as a potential mechanism of acquired resistance to BRAF inhibition in melanoma. Cancer Res 2008;68:4853–61.
42. Baumann B, Weber CK, Troppmair J, et al. Raf induces NF-κB by membrane shuttle kinase MEKK1, a signaling pathway critical for transformation. Proc Natl Acad Sci U S A 2000;97:4615–20.
43. Galaktionov K, Jessus C, Beach D. Raf1 interaction with Cdc25 phosphatase ties mitogenic signal transduction to cell cycle activation. Genes Dev 1995;9:1046–58.
44. Kerkhoff E, Rapp UR. Cell cycle targets of Ras/Raf signalling. Oncogene 1998;17:1457–62.
45. Hindley A, Kolch W. Extracellular signal regulated kinase (ERK)/mitogen activated protein kinase (MAPK)-independent functions of Raf kinases. J Cell Sci 2002;115:1575–81.
46. Liu L, Cao Y, Chen C, et al. Sorafenib blocks the RAF/MEK/ERK pathway, inhibits tumor angiogenesis, and induces tumor cell apoptosis in hepatocellular carcinoma model PLC/PRF/5. Cancer Res 2006;66:11851–8.

Addition of S-1 to the Epidermal Growth Factor Receptor Inhibitor Gefitinib Overcomes Gefitinib Resistance in Non-small cell Lung Cancer Cell Lines with *MET* Amplification

Takafumi Okabe,[1,4,5] Isamu Okamoto,[1] Sayaka Tsukioka,[7] Junji Uchida,[7] Erina Hatashita,[1] Yuki Yamada,[1] Takeshi Yoshida,[1] Kazuto Nishio,[2] Masahiro Fukuoka,[3] Pasi A. Jänne,[4,5,6] and Kazuhiko Nakagawa[1]

Abstract **Purpose:** Most non-small cell lung cancer (NSCLC) tumors with activating mutations in the epidermal growth factor receptor (EGFR) are initially responsive to EGFR tyrosine kinase inhibitors (EGFR-TKI) such as gefitinib and erlotinib, but they almost invariably develop resistance to these drugs. A secondary mutation in *EGFR* (T790M) and amplification of the *MET* proto-oncogene have been identified as mechanisms of such acquired resistance to EGFR-TKIs. We have now investigated whether addition of the oral fluoropyrimidine derivative S-1 to gefitinib might overcome gefitinib resistance in NSCLC cell lines.

Experimental Design: The effects of gefitinib on EGFR signaling and on the expression both of thymidylate synthase and of the transcription factor E2F-1 in gefitinib-resistant NSCLC cells were examined by immunoblot analysis. The effects of S-1 (or 5-fluorouracil) and gefitinib on the growth of NSCLC cells were examined *in vitro* as well as in nude mice.

Results: Gefitinib induced down-regulation of thymidylate synthase and E2F-1 in gefitinib-resistant NSCLC cells with *MET* amplification but not in those harboring the T790M mutation of *EGFR*. The combination of 5-fluorouracil and gefitinib synergistically inhibited the proliferation of cells with *MET* amplification, but not that of those with the T790M mutation of *EGFR, in vitro*. Similarly, the combination of S-1 and gefitinib synergistically inhibited the growth only of NSCLC xenografts with *MET* amplification.

Conclusions: Our results suggest that the addition of S-1 to EGFR-TKIs is a promising strategy to overcome EGFR-TKI resistance in NSCLC with *MET* amplification.

The epidermal growth factor receptor (EGFR) is a receptor tyrosine kinase that is abnormally amplified or activated in a variety of tumors, including non-small cell lung cancer (NSCLC; refs. 1-3), and it has therefore been identified as an important target in cancer treatment. Two inhibitors of the tyrosine kinase activity of EGFR (EGFR-TKI), gefitinib and erlotinib, both of which compete with ATP for binding to the tyrosine kinase pocket of the receptor, have been extensively studied in patients with NSCLC (4-7). Somatic mutations in the kinase domain of EGFR are associated with the response to EGFR-TKIs in a subset of NSCLC patients (8-15). Deletions in exon 19 of the EGFR gene (*EGFR*) and replacement of leucine with arginine at codon 858 (L858R) account for ~90% of these mutations (16-18). Despite the benefits of gefitinib and erlotinib in treatment of NSCLC associated with *EGFR* mutations, most, if not all, patients ultimately develop resistance to these drugs. In ~50% of these individuals, acquired resistance is associated with a secondary mutation, T790M, in *EGFR* (19-21). A recent study further suggested that ~20% of patients who become resistant to gefitinib do so as a result of acquired amplification of the proto-oncogene *MET* (22). The identification of strategies or agents capable of overcoming acquired resistance to EGFR-TKIs is thus an important clinical goal.

S-1 is an oral fluoropyrimidine derivative consisting of tegafur (FT) and two modulators, 5-chloro-2,4-dihydroxypyridine (gimeracil, CDHP) and potassium oxonate (oteracil, oxo), in a molar ratio of 1:0.4:1 (23, 24). S-1 is currently under evaluation for the treatment of NSCLC both as a single agent and in combination with other drugs (25-27). We have recently shown that combined treatment with S-1 and gefitinib has a synergistic antiproliferative effect on NSCLC cells regardless of the absence or presence of *EGFR* mutations (28). The gefitinib-induced down-regulation of thymidylate synthase (TS), likely mediated by down-regulation of the transcription factor E2F-1, was implicated in the synergistic antitumor effect

Authors' Affiliations: Departments of [1]Medical Oncology, [2]Genome Biology, Kinki University School of Medicine, 377-2 Ohno-higashi, Osaka-Sayama, and [3]Department of Internal Medicine, Kinki University School of Medicine, Sakai Hospital, 2-7-1 Harayamadai, Minami-ku, Sakai, Osaka, Japan; and [4]Lowe Center for Thoracic Oncology, [5]Department of Medical Oncology, Dana-Farber Cancer Institute, and [6]Department of Medicine, Brigham and Women's Hospital and Harvard Medical School, Boston, Massachusetts; and [7]Tokushima Research Center, Taiho Pharmaceutical Co. Ltd., 224-2 Hiraishi-ebisuno, Kawauchi, Tokushima, Japan

Received 8/29/08; revised 10/18/08; accepted 10/27/08.

The costs of publication of this article were defrayed in part by the payment of page charges. This article must therefore be hereby marked *advertisement* in accordance with 18 U.S.C. Section 1734 solely to indicate this fact.

Requests for reprints: Isamu Okamoto, Department of Medical Oncology, Kinki University School of Medicine, 377-2 Ohno-higashi, Osaka-Sayama, Osaka 589-8511, Japan. Phone: 81-72-366-0221; Fax: 81-72-360-5000; E-mail: chi-okamoto@dotd.med.kindai.ac.jp.

doi:10.1158/1078-0432.CCR-08-2251

Translational Relevance

Most non–small cell lung cancer (NSCLC) tumors with activating mutations in the epidermal growth factor receptor (EGFR) are initially responsive to EGFR tyrosine kinase inhibitors (EGFR-TKI) such as gefitinib and erlotinib, but they almost invariably develop resistance to these drugs. S-1 is an oral fluoropyrimidine derivative that has exhibited marked antitumor activity in recent clinical trials including patients with NSCLC. We have investigated whether the addition of S-1 to gefitinib might overcome gefitinib resistance in NSCLC cells. Gefitinib induced down-regulation of both thymidylate synthase and the transcription factor E2F-1 in gefitinib-resistant NSCLC cells with *MET* amplification but not in those harboring the T790M mutation of *EGFR*. The combination of S-1 and gefitinib exerted a synergistic antitumor effect only in gefitinib-resistant cells with *MET* amplification both *in vitro* and *in vivo*. Our preclinical findings indicate that the addition of S-1 to EGFR-TKIs is a promising strategy to overcome EGFR-TKI resistance.

of combined treatment with this EGFR-TKI and S-1. We have now examined whether treatment with gefitinib induces down-regulation of TS in gefitinib-resistant cells with *MET* amplification or the T790M mutation of *EGFR*. Moreover, we investigated the possibility that the addition of S-1 to gefitinib might overcome gefitinib resistance in NSCLC cells both *in vitro* and *in vivo*.

Materials and Methods

Cell lines and reagents. The human NSCLC cell lines HCC827, HCC827 GR5, HCC827 GR6, PC-9, PC-9/ZD, and H1975 were obtained as described previously (22, 29–31). HCC827, PC-9, PC-9/ZD, and H1975 cells were cultured under a humidified atmosphere of 5% CO_2 at 37°C in RPMI 1640 (Sigma) supplemented with 10% fetal bovine serum. HCC827 GR5 and HCC827 GR6 cells were cultured in RPMI 1640 supplemented 10% fetal bovine serum and 1 μmol/L gefitinib. Gefitinib was obtained from AstraZeneca, S-1 was provided by Taiho Pharmaceutical Co. Ltd., and 5-fluorouracil (5-FU) was from Wako.

Immunoblot analysis. Cell lysates were fractionated by SDS-PAGE on 7.5% or 12% (TS) gels, and the separated proteins were transferred to a nitrocellulose membrane. After blocking of nonspecific sites with 5% skim milk, the membrane was incubated overnight at room temperature with primary antibodies. Antibodies to phosphorylated EGFR (pY1068), to extracellular signal-regulated kinase (ERK), to phosphorylated AKT, and to AKT were obtained from Cell Signaling Technology; those to EGFR were from Zymed; those to phosphorylated ERK and to E2F-1 were from Santa Cruz Biotechnology; those to TS were from Taiho; and those to β-actin (loading control) were from Sigma. Immune complexes were detected by incubation of the membrane for 1 h at room temperature with horseradish peroxidase–conjugated goat antibodies to mouse or rabbit immunoglobulin (Amersham Biosciences) and by subsequent exposure to enhanced chemiluminescence reagents (Perkin-Elmer).

Growth inhibition assay **in vitro.** Cells (2.0×10^3) were plated in 96-well flat-bottomed plates and cultured for 24 h before incubation for 72 h in the presence of various concentrations of 5-FU and gefitinib either alone or together at a ratio of 1:5, respectively. Cell Counting kit-8 solution (Dojindo) was then added to each well, and the cells were incubated for 3 h at 37°C before measurement of absorbance at 450 nm. Data were analyzed by the median-effect method (CalcuSyn software; Biosoft) to determine the drug concentrations resulting in 50% growth inhibition (IC_{50}). The Chou and Talalay combination index (CI), a well-established index reflecting the interaction of two drugs (32), was calculated at different levels of growth inhibition with the use of CalcuSyn software. The CI for 50% growth inhibition (IC_{50}) was calculated as follows:

$$\text{CI at } IC_{50} = \frac{IC_{50}\ (5-\text{FU combination})}{IC_{50}\ (5-\text{FU alone})} + \frac{IC_{50}(\text{gefitinib combination})}{IC_{50}\ (\text{gefitinib alone})}$$

CI values of <1, 1, and >1 indicate synergistic, additive, and antagonistic effects, respectively.

Animals. Male athymic nude mice were exposed to a 12-h light, 12-h dark cycle and provided with food and water ad libitum in a barrier facility. All experiments were done in compliance with the regulations of the Animal Experimentation Committee of Taiho Pharmaceutical Co. Ltd.

Growth inhibition assay **in vivo.** Cubic fragments of tumor tissue (~2 by 2 by 2 mm) were implanted s.c. into the axilla of 5- to 6-wk-old male athymic nude mice. Treatment was initiated when tumors in each group achieved an average volume of 50 to 150 mm^3. Treatment groups consisted of control, S-1 alone, gefitinib alone, and the combination of S-1 and gefitinib. Each treatment group contained seven mice. S-1 (10 mg per kilogram of body mass) and gefitinib (3 or 50 mg/kg) were administered by oral gavage daily for 28 d; control animals received 0.5% (w/v) aqueous solution of hydroxypropylmethylcellulose as vehicle. Tumor volume was determined from caliper measurements of tumor length (L) and width (W) according to the formula $LW^2/2$. Both tumor size and body weight were measured twice or thrice per week.

Statistical analysis. Data are presented as means ± SE as indicated and were analyzed by Student's t test. A P value of <0.05 was considered statistically significant.

Results

Effects of gefitinib on TS expression in gefitinib-resistant cell lines with MET *amplification.* TS is an important target enzyme for 5-FU (33, 34), with a reduced level of TS expression having been associated with a higher rate of response to 5-FU–based chemotherapy (35, 36). We first examined the effects of gefitinib on the expression of E2F-1 and TS as well as on the phosphorylation of EGFR and downstream signaling molecules in three cell lines (HCC827, HCC827 GR5, and HCC827 GR6) by immunoblot analysis. HCC827 cells harbor the E746_A750 deletion in exon 19 of *EGFR*; HCC827 GR5 and HCC827 GR6 cells are clones of HCC827 that developed resistance to gefitinib as a result of exposure to increasing concentrations of the drug and which exhibit *MET* amplification. Gefitinib (5 μmol/L) completely inhibited both the phosphorylation of EGFR, of the protein kinase AKT, and of ERK as well as the expression of E2F-1 and TS in the parental HCC827 cells in a time-dependent manner (Fig. 1). In the resistant cells, gefitinib substantially inhibited the phosphorylation of EGFR, but it had no effect on that of AKT or ERK (Fig. 1), consistent with previous observations (22). Gefitinib induced a time-dependent decrease in the amounts of E2F-1 and TS in the resistant cells (Fig. 1). These data thus showed that gefitinib induced the down-regulation of TS expression, likely as a result of a decrease in the abundance of E2F-1, in gefitinib-resistant cells with *MET* amplification.

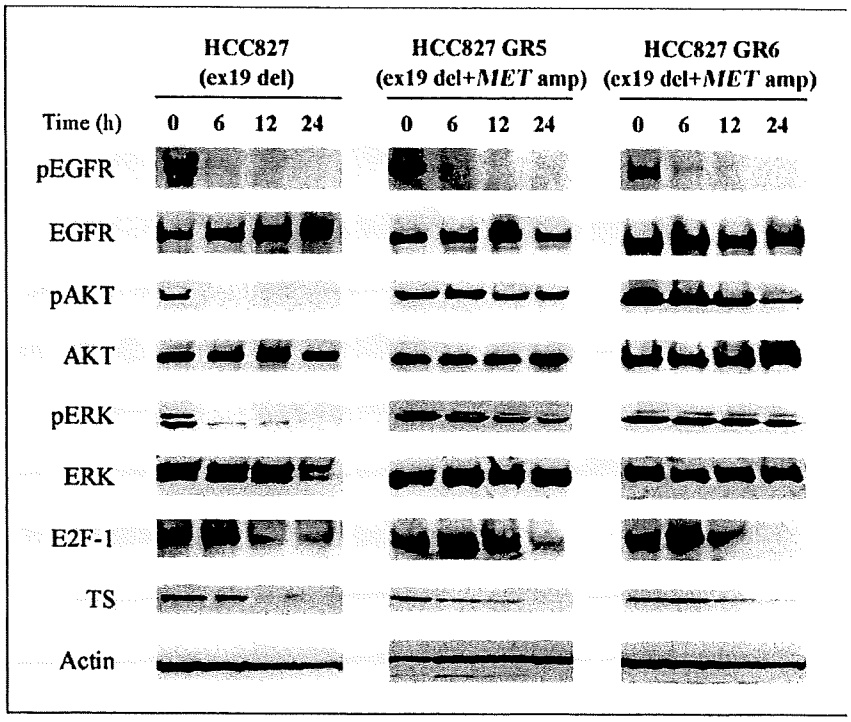

Fig. 1. Effects of gefitinib on EGFR, AKT, and ERK phosphorylation as well as on E2F-1 and TS expression in gefitinib-resistant NSCLC cells with *MET* amplification. Parental HCC827 cells and gefitinib-resistant clones with *MET* amplification (HCC827 GR5 and HCC827 GR6) were incubated with gefitinib (5 μmol/L) for the indicated times in medium containing 10% serum, after which cell lysates were subjected to immunoblot analysis with antibodies to phosphorylated (p) or total forms of EGFR, AKT, and ERK as well as with those to E2F-1, TS, and β-actin (loading control).

***Effects of gefitinib on TS expression in gefitinib-resistant cell lines with the T790M mutation of* EGFR.** We next investigated whether gefitinib might inhibit TS expression in gefitinib-resistant cells harboring the T790M mutation of *EGFR*. We examined three cell lines: PC-9, PC-9/ZD, and H1975. PC-9 cells contain the E746_A750 deletion in exon 19 of *EGFR*, whereas PC-9/ZD cells are a gefitinib-resistant clone of PC-9 and also harbor the T790M mutation of *EGFR*; H1975 cells possess both L858R and T790M mutations of *EGFR*. Gefitinib completely or almost completely inhibited the phosphorylation of EGFR, AKT, and ERK as well as the expression of E2F-1 and TS in PC-9 cells in a time-dependent manner (Fig. 2). In contrast, phosphorylation of EGFR, AKT, and ERK as well as the expression of E2F-1 and TS were maintained in PC-9/ZD and H1975 cells incubated in the presence of gefitinib (Fig. 2). These findings thus showed that gefitinib failed to inhibit the expression of TS in gefitinib-resistant cells with a secondary T790M mutation of *EGFR*.

***Effects of the combination of 5-FU and gefitinib on the growth of gefitinib-resistant cell lines* in vitro.** We next investigated whether the down-regulation of TS expression induced by gefitinib in gefitinib-resistant cells with *MET* amplification would render these cells sensitive to the synergistic antiproliferative effect of the combination of S-1 and gefitinib. We therefore first examined the antiproliferative activity of the combination of 5-FU and gefitinib in the four gefitinib-resistant cell lines (HCC827 GR5, HCC827 GR6, PC-9/ZD, and H1975) *in vitro*. We used 5-FU instead of S-1 for *in vitro* experiments because tegafur, which is a component of S-1, is metabolized to 5-FU primarily in the liver. The combined effect of 5-FU and gefitinib was evaluated on the basis of the CI. The combination of 5-FU and gefitinib induced a synergistic growth-inhibitory effect (CI < 1) in cells with *MET* amplification, yielding CI values of 0.87 and 0.78 at 50% growth inhibition for HCC827 GR5 and HCC827 GR6 cells, respectively (Table 1; Fig. 3). In contrast, an antagonistic interaction (CI > 1) between 5-FU and gefitinib was apparent for cells harboring the T790M mutation of *EGFR*, with CIs of 1.10 and 1.42 at 50% growth inhibition for PC-9/ZD and H1975 cells, respectively (Table 1; Fig. 3). These results thus showed that the combination of 5-FU and gefitinib had a synergistic effect in gefitinib-resistant cells with *MET* amplification but not in those with the T790M mutation of *EGFR*.

***Effects of combined treatment with S-1 and gefitinib on the growth of gefitinib- resistant cell lines* in vivo.** We next investigated whether combined treatment with S-1 and gefitinib exhibited a synergistic effect on the growth of gefitinib-resistant cells with *MET* amplification *in vivo*. Doses of the two agents were selected to ensure moderate independent effects on tumor growth. When the tumors become palpable (50-150 mm^3), mice were divided into four groups and treated with vehicle, S-1, gefitinib, or the combination of both drugs by oral gavage for 4 wk. Combination therapy with S-1 and gefitinib inhibited the growth of tumors formed by PC-9 cells to a significantly greater extent than did treatment with S-1 or gefitinib alone (Fig. 4*A*). In contrast, no such synergistic effect was observed with tumors formed by PC-9/ZD (Fig. 4*B*) or H1975 (Fig. 4*C*) cells. Given that TS expression was inhibited by gefitinib in PC-9 cells but not in the gefitinib-resistant clone PC-9/ZD or in H1975 cells, these data suggested that the down-regulation of TS by gefitinib was responsible, at least in part, for the synergistic antitumor effect of S-1 and gefitinib. We then examined the effects of S-1 and gefitinib on the growth of HCC827 GR5 tumor xenografts with *MET* amplification. Neither S-1 nor gefitinib alone had a substantial effect on tumor growth (Fig. 4*D*). In contrast, administration of the two agents together resulted in a synergistic and almost complete inhibition of tumor growth (Fig. 4*D*). All of the treatments were well-tolerated, with no signs of toxicity or

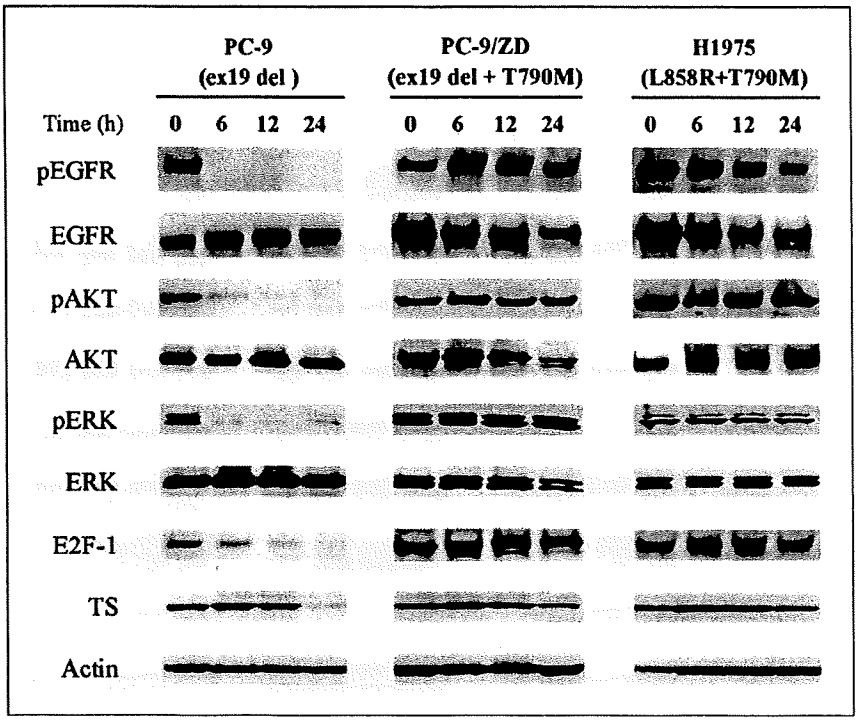

Fig. 2. Effects of gefitinib on EGFR, AKT, and ERK phosphorylation as well as on E2F-1 and TS expression in gefitinib-resistant NSCLC cells with the T790M mutation of *EGFR*. PC-9 cells as well as the gefitinib-resistant lines PC-9/ZD and H1975 harboring the T790M mutation of *EGFR* were incubated with gefitinib (5 μmol/L) for the indicated times in medium containing 10% serum, after which cell lysates were subjected to immunoblot analysis as in Fig. 1.

weight loss during therapy (data not shown). These findings suggested that combination treatment with S-1 and gefitinib had a synergistic antitumor effect *in vivo* with gefitinib-resistant xenografts manifesting *MET* amplification, but not with those harboring the T790M mutation of *EGFR*, consistent with the results obtained *in vitro*.

Discussion

We have previously shown that combination treatment with S-1 and gefitinib had a synergistic antiproliferative effect on NSCLC cells regardless of the absence or presence of *EGFR* mutations, with down-regulation of TS by gefitinib contributing to its synergistic interaction with S-1 (28). In the present study, we examined whether gefitinib induces down-regulation of TS expression in NSCLC cell lines with different mechanisms of resistance to EGFR-TKIs. We used a gefitinib concentration of 5 μmol/L for these *in vitro* experiments. The concentration of gefitinib in tumor xenografts was previously shown to be 5 to 14 times that in plasma of mouse hosts treated with this drug (37). Daily oral administration of gefitinib (250 mg) in patients also gave rise to a drug concentration in tumor tissue that was substantially higher (by a mean factor of 42) than that in plasma (37). We previously showed that the maximal concentration of gefitinib in plasma of patients with advanced solid tumors had a mean value of 0.76 μmol/L at a daily dose of 225 mg (38). On the basis of these observations, a gefitinib concentration of 5 μmol/L is similar to the achievable concentration in tumor tissue of treated humans. We found that gefitinib inhibited TS expression in association with E2F-1 down-regulation in gefitinib-resistant cells with *MET* amplification but not in those with the T790M mutation of *EGFR*. One possible explanation for this difference in response between cells with *MET* amplification and those with the T790M mutation of *EGFR* is that gefitinib inhibited EGFR phosphorylation in the former cells but not in the latter. The T790M mutation is thought to inhibit the ability of gefitinib or erlotinib to bind to the ATP-binding pocket of the catalytic

Table 1. IC_{50} and CI values for the antiproliferative effects of gefitinib and 5-FU, alone or combined, on the growth of NSCLC cells *in vitro*

	Alone IC_{50} (μmol/L)		Combination IC_{50} (μmol/L)*		CI at IC_{50}
	Gefitinib	5-FU	Gefitinib	5-FU	
HCC827 GR5	11.64	2.83	5.56	1.11	0.87
HCC827 GR6	14.44	4.90	7.11	1.42	0.78
PC9/ZD	9.13	8.66	8.33	1.67	1.10
H1975	34.82	11.67	30.98	6.20	1.42

NOTE: Data are means of triplicates from a representative experiment.
*The concentrations of the two drugs needed to inhibit cell growth by 50% when gefitinib and 5-FU are combined.

domain of the receptor (19, 20), with the result that these agents are not able to suppress the phosphorylation of EGFR. *MET* amplification confers EGFR-TKI resistance by activating ErbB3 signaling in an EGFR-independent manner (22). Given that the increased affinity of EGFR for gefitinib conferred by primary *EGFR* mutations is maintained in cells with *MET* amplification, gefitinib is still able to inhibit EGFR phosphorylation in such cells (22). These observations raise the possibility that gefitinib-induced down-regulation of TS is determined by modulation of EGFR phosphorylation. On the other hand, the phosphorylation of AKT and ERK was not blocked by gefitinib in cells with the T790M mutation of *EGFR* or those with *MET* amplification, suggesting that the expression of TS might be regulated by an EGFR signaling pathway other than that mediated by AKT and ERK.

We evaluated the effects of combined treatment with S-1 and gefitinib on the proliferation of NSCLC cells with the two different types of gefitinib resistance mechanism. We found that S-1 (or 5-FU) and gefitinib exerted a synergistic antiproliferative effect in NSCLC cells with *MET* amplification both *in vitro* and *in vivo*, but that no such effect was apparent with cells harboring the T790M mutation of *EGFR*. These observations were consistent with the gefitinib-induced down-regulation of TS observed in the former cells but not in the latter. The active metabolite of 5-FU, fluoro-dUMP, forms a covalent complex with TS, resulting in inhibition of DNA synthesis (33, 34). TS is thus an important therapeutic target of 5-FU. An increase in TS expression and activity has been viewed as a mechanistic driver of 5-FU resistance in cancer cells (39–41). Down-regulation of TS would thus be expected to enhance the cytotoxicity of 5-FU as a result of the decrease in the amount of its protein target (42). Indeed, preclinical studies have shown that the down-regulation of TS by antisense oligonucleotides or other means enhances the efficacy of 5-FU (43–46), supporting the notion that gefitinib-induced down-regulation of TS contributes to its synergistic interaction with S-1 in gefitinib-resistant NSCLC cells with *MET* amplification.

A recent clinical study showed that most patients with acquired resistance to gefitinib or erlotinib manifested a worsening of lung cancer symptoms and an increase in tumor size after discontinuation of these agents (47). However, most of these individuals showed stabilization or improvement in symptoms and a decrease in tumor size on resumption of EGFR-TKI treatment (47). These clinical findings suggest the possibility that tumors with acquired resistance to EGFR-TKIs continue to require signaling through EGFR for their survival. Indeed, a preclinical study found that the combination of gefitinib and an inhibitor of the tyrosine kinase activity of MET, but neither agent alone, induced substantial growth inhibition in gefitinib-resistant NSCLC cells with *MET* amplification (22). These observations support the notion that the continuation of treatment with gefitinib or erlotinib might be of value even after the development of acquired resistance to these drugs. Our present results indicate that the addition of S-1 to EGFR-TKIs might overcome EGFR-TKI resistance in patients whose resistance is attributable to *MET* amplification.

The T790M mutation of *EGFR* and *MET* amplification account for ~60% to 70% of all cases of acquired resistance to gefitinib or erlotinib (19–22). A signaling pathway dependent on the insulin-like growth factor receptor was also recently implicated in resistance to EGFR-TKIs (48). The mechanisms of EGFR-TKI resistance other than that mediated by the T790M mutation of *EGFR* may thus be dependent on the activation of receptor tyrosine kinases that are not directly targeted by these drugs. Given that gefitinib would be expected to inhibit EGFR phosphorylation in all gefitinib-resistant cells with such a mechanism of resistance, treatment with this drug might also be expected to induce the down-regulation of TS

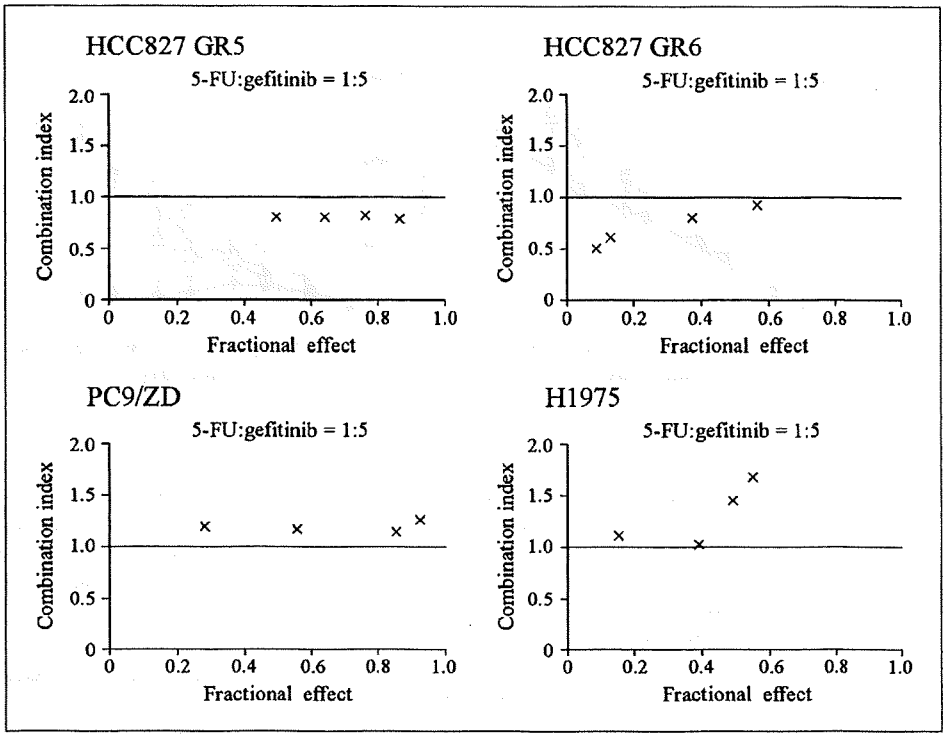

Fig. 3. Effects of the combination of 5-FU and gefitinib on the growth of gefitinib-resistant NSCLC cells *in vitro*. Cells with *MET* amplification (HCC827 GR5 and HCC827 GR6) or those harboring the T790M mutation of *EGFR* (PC-9/ZD and H1975) were incubated for 72 h with 5-FU or gefitinib alone or with both drugs at a fixed 5-FU:gefitinib molar ratio of 1:5, after which cell viability was measured. The interaction between 5-FU and gefitinib was evaluated on the basis of the CI, which is plotted against the fraction of growth inhibition. Data are means of triplicates from a representative experiment.

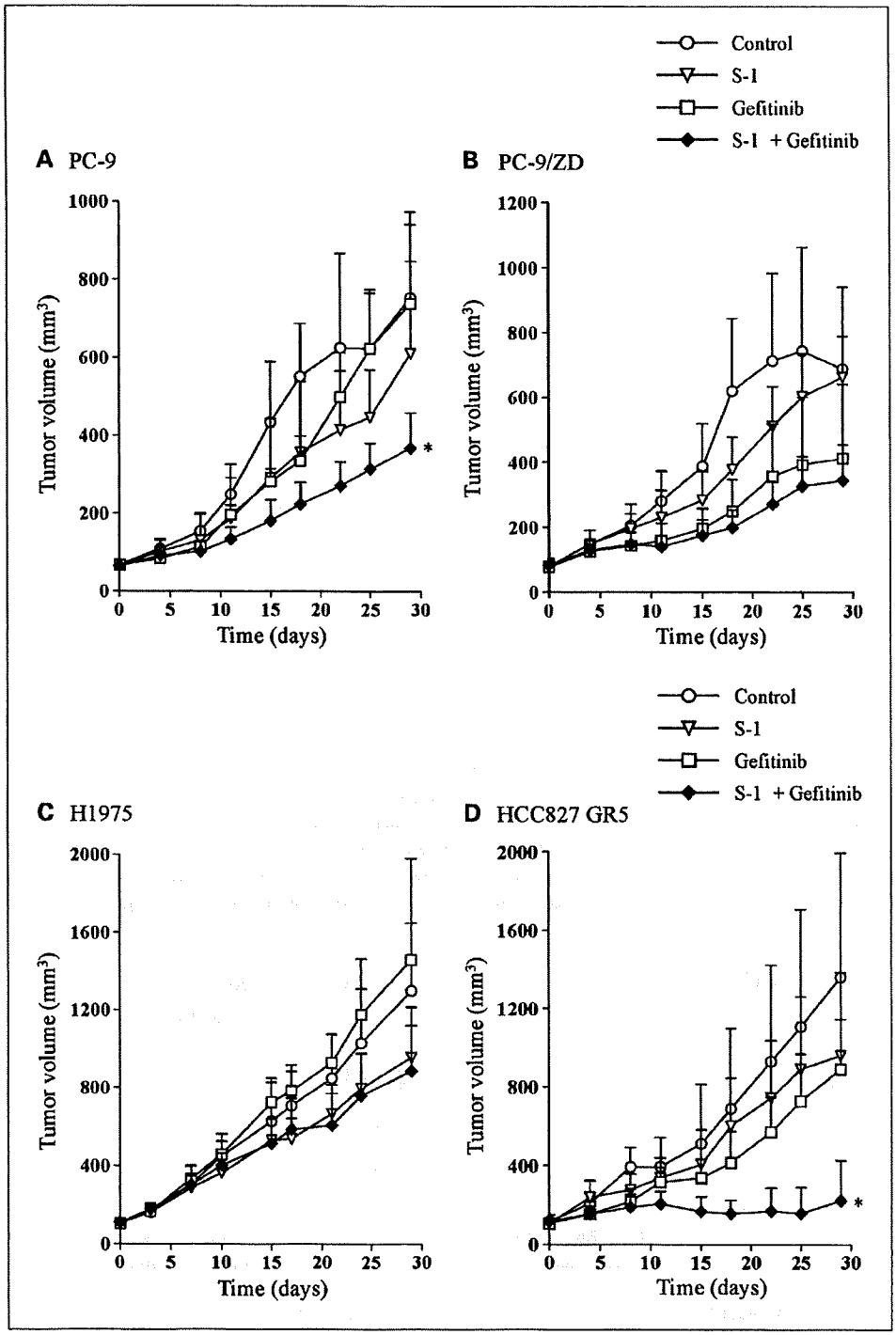

Fig. 4. Effects of the combination of S-1 and gefitinib on the growth of gefitinib-resistant NSCLC cells *in vivo*. *A*, nude mice with tumor xenografts established by s.c. implantation of PC-9 cells were treated daily for 4 wk with vehicle (control), S-1 (10 mg/kg), gefitinib (3 mg/kg), or both drugs by oral gavage. *B* to *D*, nude mice with tumor xenografts of NSCLC cells either harboring theT790M mutation of *EGFR* (PC-9/ZD and H1975) or exhibiting *MET* amplification (HCC827 GR5) were treated daily for 4 wk with vehicle (control), S-1 (10 mg/kg), gefitinib (50 mg/kg), or both drugs by oral gavage. Tumor volume was determined at the indicated times after the onset of treatment. *Points*, mean of values from seven mice per group; *bars*, SE. *, $P < 0.05$ for the combination of S-1 plus gefitinib versus control or either S-1 or gefitinib alone (Student's *t* test).

expression that facilitates the antitumor effect of S-1. Pemetrexed, an antifolate drug with multiple targets, has also shown antitumor activity mediated by TS inhibition in a broad range of tumors including NSCLC (49–53). The addition of S-1 or pemetrexed to gefitinib may thus prove effective in NSCLC patients whose gefitinib resistance is attributable to activation of a non-EGFR tyrosine kinase.

In conclusion, we have shown that the combination of S-1 and gefitinib had a synergistic antiproliferative effect in gefitinib-resistant NSCLC cells with *MET* amplification. The inhibition of EGFR phosphorylation and down-regulation of TS by gefitinib were associated with the synergistic interaction between gefitinib and S-1. Our preclinical results suggest that the addition of S-1 to gefitinib is a potential strategy for overcoming EGFR-TKI resistance and warrants clinical evaluation.

Disclosure of Potential Conflicts of Interest

No potential conflicts of interest were disclosed.

References

1. Ritter CA, Arteaga CL. The epidermal growth factor receptor-tyrosine kinase: a promising therapeutic target in solid tumors. Semin Oncol 2003;30:3–11.
2. Hirsch FR, Varella-Garcia M, Bunn PA, Jr., et al. Epidermal growth factor receptor in non-small-cell lung carcinomas: correlation between gene copy number and protein expression and impact on prognosis. J Clin Oncol 2003;21:3798–807.
3. Suzuki S, Dobashi Y, Sakurai H, Nishikawa K, Hanawa M, Ooi A. Protein overexpression and gene amplification of epidermal growth factor receptor in nonsmall cell lung carcinomas. An immunohistochemical and fluorescence *in situ* hybridization study. Cancer 2005;103:1265–73.
4. Fukuoka M, Yano S, Giaccone G, et al. Multi-institutional randomized phase II trial of gefitinib for previously treated patients with advanced non-small-cell lung cancer (The IDEAL 1 Trial) [corrected]. J Clin Oncol 2003;21:2237–46.
5. Perez-Soler R, Chachoua A, Hammond LA, et al. Determinants of tumor response and survival with erlotinib in patients with non-small-cell lung cancer. J Clin Oncol 2004;22:3238–47.
6. Thatcher N, Chang A, Parikh P, et al. Gefitinib plus best supportive care in previously treated patients with refractory advanced non-small-cell lung cancer: results from a randomised, placebo-controlled, multicentre study (Iressa Survival Evaluation in Lung Cancer). Lancet 2005;366:1527–37.
7. Shepherd FA, Rodrigues Pereira J, Ciuleanu T, et al. Erlotinib in previously treated non-small-cell lung cancer. N Engl J Med 2005;353:123–32.
8. Lynch TJ, Bell DW, Sordella R, et al. Activating mutations in the epidermal growth factor receptor underlying responsiveness of non-small-cell lung cancer to gefitinib. N Engl J Med 2004;350:2129–39.
9. Paez JG, Janne PA, Lee JC, et al. EGFR mutations in lung cancer: correlation with clinical response to gefitinib therapy. Science 2004;304:1497–500.
10. Pao W, Miller V, Zakowski M, et al. EGF receptor gene mutations are common in lung cancers from never smokers and are associated with sensitivity of tumors to gefitinib and erlotinib. Proc Natl Acad Sci U S A 2004;101:13306–11.
11. Mitsudomi T, Kosaka T, Endoh H, et al. Mutations of the epidermal growth factor receptor gene predict prolonged survival after gefitinib treatment in patients with non-small-cell lung cancer with postoperative recurrence. J Clin Oncol 2005;23:2513–20.
12. Takano T, Ohe Y, Sakamoto H, et al. Epidermal growth factor receptor gene mutations and increased copy numbers predict gefitinib sensitivity in patients with recurrent non-small-cell lung cancer. J Clin Oncol 2005;23:6829–37.
13. Han SW, Kim TY, Hwang PG, et al. Predictive and prognostic impact of epidermal growth factor receptor mutation in non-small-cell lung cancer patients treated with gefitinib. J Clin Oncol 2005;23:2493–501.
14. Tsao MS, Sakurada A, Cutz JC, et al. Erlotinib in lung cancer-molecular and clinical predictors of outcome. N Engl J Med 2005;353:133–44.
15. Tokumo M, Toyooka S, Kiura K, et al. The relationship between epidermal growth factor receptor mutations and clinicopathologic features in non-small cell lung cancers. Clin Cancer Res 2005;11:1167–73.
16. Kosaka T, Yatabe Y, Endoh H, Kuwano H, Takahashi T, Mitsudomi T. Mutations of the epidermal growth factor receptor gene in lung cancer: biological and clinical implications. Cancer Res 2004;64:8919–23.
17. Shigematsu H, Lin L, Takahashi T, et al. Clinical and biological features associated with epidermal growth factor receptor gene mutations in lung cancers. J Natl Cancer Inst 2005;97:339–46.
18. Sharma SV, Bell DW, Settleman J, Haber DA. Epidermal growth factor receptor mutations in lung cancer. Nat Rev Cancer 2007;7:169–81.
19. Kobayashi S, Boggon TJ, Dayaram T, et al. EGFR mutation and resistance of non-small-cell lung cancer to gefitinib. N Engl J Med 2005;352:786–92.
20. Pao W, Miller VA, Politi KA, et al. Acquired resistance of lung adenocarcinomas to gefitinib or erlotinib is associated with a second mutation in the EGFR kinase domain. PLoS Med 2005;2:e73.
21. Kosaka T, Yatabe Y, Endoh H, et al. Analysis of epidermal growth factor receptor gene mutation in patients with non-small cell lung cancer and acquired resistance to gefitinib. Clin Cancer Res 2006;12:5764–9.
22. Engelman JA, Zejnullahu K, Mitsudomi T, et al. MET amplification leads to gefitinib resistance in lung cancer by activating ERBB3 signaling. Science 2007;316:1039–43.
23. Shirasaka T, Shimamoto Y, Fukushima M. Inhibition by oxonic acid of gastrointestinal toxicity of 5-fluorouracil without loss of its antitumor activity in rats. Cancer Res 1993;53:4004–9.
24. Shirasaka T, Nakano K, Takechi T, et al. Antitumor activity of 1 M tegafur-0.4 M 5-chloro-2,4-dihydroxypyridine-1 M potassium oxonate (S-1) against human colon carcinoma orthotopically implanted into nude rats. Cancer Res 1996;56:2602–6.
25. Kawahara M, Furuse K, Segawa Y, et al. Phase II study of S-1, a novel oral fluorouracil, in advanced non-small-cell lung cancer. Br J Cancer 2001;85:939–43.
26. Ichinose Y, Yoshimori K, Sakai H, et al. S-1 plus cisplatin combination chemotherapy in patients with advanced non-small cell lung cancer: a multi-institutional phase II trial. Clin Cancer Res 2004;10:7860–4.
27. Okamoto I, Nishimura T, Miyazaki M, et al. Phase II study of combination therapy with S-1 and irinotecan for advanced non-small cell lung cancer: West Japan Thoracic Oncology Group 3505. Clin Cancer Res 2008;14:5250–4.
28. Okabe T, Okamoto I, Tsukioka S, et al. Synergistic antitumor effect of S-1 and the epidermal growth factor receptor inhibitor gefitinib in non-small cell lung cancer cell lines: role of gefitinib-induced down-regulation of thymidylate synthase. Mol Cancer Ther 2008;7:599–606.
29. Mukohara T, Engelman JA, Hanna NH, et al. Differential effects of gefitinib and cetuximab on non-small-cell lung cancers bearing epidermal growth factor receptor mutations. J Natl Cancer Inst 2005;97:1185–94.
30. Okabe T, Okamoto I, Tamura K, et al. Differential constitutive activation of the epidermal growth factor receptor in non-small cell lung cancer cells bearing EGFR gene mutation and amplification. Cancer Res 2007;67:2046–53.
31. Koizumi F, Shimoyama T, Taguchi F, Saijo N, Nishio K. Establishment of a human non-small cell lung cancer cell line resistant to gefitinib. Int J Cancer 2005;116:36–44.
32. Chou TC, Talalay P. Quantitative analysis of dose-effect relationships: the combined effects of multiple drugs or enzyme inhibitors. Adv Enzyme Regul 1984;22:27–55.
33. Berger SH, Berger FG. Thymidylate synthase as a determinant of 5-fluoro-2'-deoxyuridine response in human colonic tumor cell lines. Mol Pharmacol 1988;34:474–9.
34. Peters GJ, van der Wilt CL, van Triest B, et al. Thymidylate synthase and drug resistance. Eur J Cancer 1995;31A:1299–305.
35. Salonga D, Danenberg KD, Johnson M, et al. Colorectal tumors responding to 5-fluorouracil have low gene expression levels of dihydropyrimidine dehydrogenase, thymidylate synthase, and thymidine phosphorylase. Clin Cancer Res 2000;6:1322–7.
36. Ichikawa W, Uetake H, Shirota Y, et al. Combination of dihydropyrimidine dehydrogenase and thymidylate synthase gene expressions in primary tumors as predictive parameters for the efficacy of fluoropyrimidine-based chemotherapy for metastatic colorectal cancer. Clin Cancer Res 2003;9:786–91.
37. McKillop D, Partridge EA, Kemp JV, et al. Tumor penetration of gefitinib (Iressa), an epidermal growth factor receptor tyrosine kinase inhibitor. Mol Cancer Ther 2005;4:641–9.
38. Nakagawa K, Tamura T, Negoro S, et al. Phase I pharmacokinetic trial of the selective oral epidermal growth factor receptor tyrosine kinase inhibitor gefitinib ('Iressa', ZD1839) in Japanese patients with solid malignant tumors. Ann Oncol 2003;14:922–30.
39. Johnston PG, Drake JC, Trepel J, Allegra CJ. Immunological quantitation of thymidylate synthase using the monoclonal antibody TS 106 in 5-fluorouracil-sensitive and -resistant human cancer cell lines. Cancer Res 1992;52:4306–12.
40. Copur S, Aiba K, Drake JC, Allegra CJ, Chu E. Thymidylate synthase gene amplification in human colon cancer cell lines resistant to 5-fluorouracil. Biochem Pharmacol 1995;49:1419–26.
41. Kawate H, Landis DM, Loeb LA. Distribution of mutations in human thymidylate synthase yielding resistance to 5-fluorodeoxyuridine. J Biol Chem 2002;277:36304–11.
42. Ferguson PJ, Collins O, Dean NM, et al. Antisense down-regulation of thymidylate synthase to suppress growth and enhance cytotoxicity of 5-FUdR, 5-FU and Tomudex in HeLa cells. Br J Pharmacol 1999;127:1777–86.
43. Hsueh CT, Kelsen D, Schwartz GK. UCN-01 suppresses thymidylate synthase gene expression and enhances 5-fluorouracil-induced apoptosis in a sequence-dependent manner. Clin Cancer Res 1998;4:2201–6.
44. Ju J, Kane SE, Lenz HJ, Danenberg KD, Chu E, Danenberg PV. Desensitization and sensitization of cells to fluoropyrimidines with different antisenses directed against thymidylate synthase messenger RNA. Clin Cancer Res 1998;4:2229–36.
45. Lee JH, Park JH, Jung Y, et al. Histone deacetylase inhibitor enhances 5-fluorouracil cytotoxicity by down-regulating thymidylate synthase in human cancer cells. Mol Cancer Ther 2006;5:3085–95.
46. Wada Y, Yoshida K, Suzuki T, et al. Synergistic effects of docetaxel and S-1 by modulating the expression of metabolic enzymes of 5-fluorouracil in human gastric cancer cell lines. Int J Cancer 2006;119:783–91.
47. Riely GJ, Kris MG, Zhao B, et al. Prospective assessment of discontinuation and reinitiation of erlotinib or gefitinib in patients with acquired resistance to erlotinib or gefitinib followed by the addition of everolimus. Clin Cancer Res 2007;13:5150–5.
48. Guix M, Faber AC, Wang SE, et al. Acquired resistance to EGFR tyrosine kinase inhibitors in cancer cells is mediated by loss of IGF-binding proteins. J Clin Invest 2008;118:2609–19.
49. Shih C, Chen VJ, Gossett LS, et al. LY231514, a pyrrolo[2,3-d]pyrimidine-based antifolate that inhibits multiple folate-requiring enzymes. Cancer Res 1997;57:1116–23.
50. John W, Picus J, Blanke CD, et al. Activity of multitargeted antifolate (pemetrexed disodium, LY231514) in patients with advanced colorectal carcinoma: results from a phase II study. Cancer 2000;88:1807–13.
51. Vogelzang NJ, Rusthoven JJ, Symanowski J, et al. Phase III study of pemetrexed in combination with cisplatin versus cisplatin alone in patients with malignant pleural mesothelioma. J Clin Oncol 2003;21:2636–44.
52. Hanna N, Shepherd FA, Fossella FV, et al. Randomized phase III trial of pemetrexed versus docetaxel in patients with non-small-cell lung cancer previously treated with chemotherapy. J Clin Oncol 2004;22:1589–97.
53. Adjei AA. Pemetrexed (ALIMTA), a novel multitargeted antineoplastic agent. Clin Cancer Res 2004;10:4276–80s.

Int. J. Cancer: **124,** 1072–1080 (2009)

SRPX2 is overexpressed in gastric cancer and promotes cellular migration and adhesion

Kaoru Tanaka[1,2], Tokuzo Arao[1], Mari Maegawa[1], Kazuko Matsumoto[1], Hiroyasu Kaneda[1,2], Kanae Kudo[1], Yoshihiko Fujita[1], Hideyuki Yokote[1], Kazuyoshi Yanagihara[3], Yasuhide Yamada[4], Isamu Okamoto[2], Kazuhiko Nakagawa[2] and Kazuto Nishio[1]*

[1]*Department of Genome Biology, Kinki University School of Medicine, Osaka-Sayama, Osaka, Japan*
[2]*Department of Medical Oncology, Kinki University School of Medicine, Osaka-Sayama, Osaka, Japan*
[3]*Central Animal Lab, National Cancer Center Research Institute, Chuo-ku, Tokyo, Japan*
[4]*Department of Medical Oncology, National Cancer Center Hospital, Chuo-ku, Tokyo, Japan*

SRPX2 **(Sushi repeat containing protein, X-linked 2) was first identified as a downstream molecule of the *E2A-HLF* fusion gene in t(17;19)-positive leukemia cells and the biological function of this gene remains unknown. We found that *SRPX2* is overexpressed in gastric cancer and the expression and clinical features showed that high mRNA expression levels were observed in patients with unfavorable outcomes using real-time RT-PCR. The cellular distribution of SRPX2 protein showed the secretion of SRPX2 into extracellular regions and its localization in the cytoplasm. The introduction of the *SRPX2* gene into HEK293 cells did not modulate the cellular proliferative activity but did enhance the cellular migration activity, as shown using migration and scratch assays. The conditioned-medium obtained from SRPX2-overexpressing cells increased the cellular migration activity of a gastric cancer cell line, SNU-16. In addition, SRPX2 protein remarkably enhanced the cellular adhesion of SNU-16 and HSC-39 and increased the phosphorylation levels of focal adhesion kinase (FAK), as shown using western blotting, suggesting that SRPX2 enhances cellular migration and adhesion through FAK signaling. In conclusion, the overexpression of SRPX2 enhances cellular migration and adhesion in gastric cancer cells. Here, we report that the biological functions of SRPX2 include cellular migration and adhesion to cancer cells.**
© *2008 Wiley-Liss, Inc.*

Key words: SRPX2; gastric cancer; cellular adhesion; cellular migration

SRPX2 (Sushi repeat containing protein, X-linked 2) was first identified as *SRPUL* (Sushi repeat protein upregulated in leukemia) by Kurosawa *et al.*[1] The *E2A-HLF* fusion gene causes B-cell precursor acute lymphoblastic leukemia, which is characterized by an unusual paraneoplastic syndrome comprising intravascular coagulation and hypercalcemia; one of the target genes of *E2A-HLF* is *SRPX2*. Apart from the possible involvement of this gene in malignant diseases, a disease-causing mutation (p.N327S) in *SRPX2* resulting in a gain-of-glycosylation aberration in the secreted mutant protein, and the mutation actually leads to rolandic epilepsy with oral and speech dyspraxia and with mental retardation in the French family.[2] While a second mutation (p.Y72S) leads to rolandic epilepsy with bilateral perisylvian polymicrogyria in another family.[3] The involvement of *SRPX2* in these disorders suggests an important role for *SRPX2* in the perisylvian region, which is critical for language and cognitive development.

SRPX2 contains 3 sushi domains and 1 hyaline domain. A sushi domain, also known as a complement control protein module or a short complement-like repeat, contains ~60 amino acids and is found in functionally diverse proteins, such as regulators of the complement activation family, GABA receptor, thyroid peroxidase and selectin family.[4,5] Sushi domains are thought to mediate specific protein–protein or protein–carbohydrate binding and cellular adhesive functions.[4] A phylogenetic analysis revealed that *SRPX2* belongs to a family of 5 genes: *SRPX2*, *SRPX*, *SELP* (selectin P precursor), *SELE* (selectin E precursor) and *SVEP1* (selectin-like protein).[3] *SRPX/SRPX1/EXT1/DRS* has the highest degree of similarity and may be involved in X-linked retinitis pigmentosa.[6,7] The selectin family, which is well known for its biological roles in leukocyte migration, cellular attachment and rolling, also contains sushi domain repeats and are phylogenetic similar to *SRPX2*.[3]

SRPX2 also contains a hyaline (HYR) domain, and this domain probably corresponds to a new superfamily in the immunoglobulin fold. The HYR domains are often associated with sushi domains, and although the function of HYR domains is uncertain, it is thought to be involved in cellular adhesion.[8] Thus, accumulating data on the motifs found in *SRPX2* suggest that *SRPX2* may be involved in cellular adhesion.

We previously performed a microarray analysis of paired clinical samples of gastric cancer and noncancerous lesions obtained from gastric cancer patients[9] and found that *SRPX2* is overexpressed in gastric cancer tissue. The present study sought to clarify the biological function of *SRPX2* expression in gastric cancer.

Material and methods

Cell culture

HEK293 (human embryonic kidney cell line) was maintained in DMEM medium, and SNU-16, HSC-39, 44As3, HSC-43, HSC-44, MKN1 and MKN7 (human gastric cancer cell lines) were maintained in RPMI1640 medium (Sigma, St. Louis, MO) supplemented with 10% FBS (GIBCO BRL, Grand Island, NY). HUVEC (human umbilical vein endothelial cells) was maintained in Humedia-EG2 (KURABO, Tokyo, Japan) medium with 1% FBS under the addition of epidermal growth factor and fibroblast growth factor.

Expression vector construction and viral production

The full-length cDNA fragment encoding human *SRPX2* was obtained from 44As3 cells using RT-PCR and the following primers: SRPX2-F, CGG GAT CCT CAA GGA TGG CCA GTC AGC TAA CTC AAA GAG G; SRPX2-R, CCC AAG CTT GGG CTC GCA TAT GTC CCT TTG CTC CCG ACG CTG GG. The sequences of the PCR-amplified DNAs were confirmed by sequencing after cloning into a pCR-Blunt II-TOPO cloning vector (Invitrogen, Carlsbad, CA). *SRPX2* cDNA was fused to a GFP-containing pcDNA3.1 vector (Clontech, Palo Alt, CA). Empty, GFP and SRPX2-GFP vectors were then transfected into HEK293 cells using FuGENE6 transfection reagent (Roche Diagnostics, Basel, Switzerland). Hygromycin selection (100 μg/mL) was

Grant sponsors: Third-Term Comprehensive 10-Year Strategy for Cancer Control, The Program for the Promotion of Fundamental Studies in Health Sciences of the National Institute of Biomedical Innovation (NiBio), The Japan Health Sciences Foundation.
***Correspondence to:** Department of Genome Biology, Kinki University School of Medicine, 377-2 Ohno-higashi, Osaka-Sayama, Osaka 589-8511, Japan. Fax: +81-72-366-0206. E-mail: knishio@med.kindai.ac.jp
Received 18 June 2008; Accepted after revision 22 September 2008
DOI 10.1002/ijc.24065
Published online 22 October 2008 in Wiley InterScience (www.interscience.wiley.com).

performed on days 2–8 after transfection, and then the cells were cultured in normal medium for another 10 days. The vectors and stable transfectant HEK293 cells were designated as pcDNA-mock, pcDNA-GFP, pcDNA-SRPX2/GFP, HEK293-pcDNA-mock, HEK293-pcDNA-GFP and HEK293-pcDNA-SRPX2/GFP.

SRPX2 cDNA in pcDNA3.1 vector was cut out and transferred into a pQCLIN retroviral vector (BD Biosciences Clontech, San Diego, CA) together with enhanced green fluorescent protein (EGFP) following internal ribosome entry site sequence (IRES) to monitor the expression of the inserts indirectly. A pVSV-G vector (Clontech, Palo Alt, CA) for the constitution of the viral envelope and the pQCXIX constructs were cotransfected into the GP2-293 cells using FuGENE6 transfection reagent. Briefly, 80% confluent cells cultured on a 10-cm dish were transfected with 2 μg pVSV-G plus 6 μg pQCXIX vectors. After 48 hr of transfection, the culture medium was collected and the viral particles were concentrated by centrifugation at 15,000*g* for 3 hr at 4°C. The viral pellet was then resuspended in fresh RPMI1640 medium. The titer of the viral vector was calculated by counting the EGFP-positive cells that were infected by serial dilutions of virus-containing media, and the multiplicity of infection (MOI) was then determined. The viral vector and stable viral transfectant cells in each cell line were designated as pQCLIN-EGFP, pQCLIN-SRPX2, HEK293-pQCLIN-EGFP, HEK293-pQCLIN-SRPX2, MKN1-pQCLIN-EGFP and MKN1-pQCLIN-SRPX2.

Patients and samples

An analysis of *SRPX2* expression levels and clinical features was performed using data from patients aged 20 to 75 years and with histologically confirmed, Stage IV gastric cancer. Additional inclusion criteria included an Eastern Cooperative Oncology Group performance status of 0–2. The exclusion criteria included prior chemotherapy or major surgery. Fifty-seven gastric cancer samples were evaluated in this study. All the patients received chemotherapy after registration and endoscopical biopsy. Gastric cancer and noncancerous gastric mucosa samples were evaluated for *SRPX2* expression in the first consecutive 24 patients. This study was approved by the institutional review board of the National Cancer Center Hospital, and written informed consent was obtained from all the patients. Endoscopic biopsy samples were immediately placed in an RNA stabilization solution (Isogen; Nippongene, Tokyo, Japan) and stored at −80°C. Other biopsy samples obtained from the same location were reviewed by a pathologist to confirm the presence of tumor cells. The RNA extraction method and the quality check protocol have been previously described.[10]

Real-time reverse-transcription PCR

One microgram of total RNA from normal tissue purchased from Clontech and from a cultured cell line was converted to cDNA using a GeneAmp® RNA-PCR kit (Applied Biosystems, CA). Real-time PCR was carried out using the Applied Biosystems 7900HT Fast Real-time PCR System (Applied Biosystems) under the following conditions: 95°C for 6 min, 40 cycles of 95°C for 15 sec and 60°C for 1 min. Glyceraldehyde 3 phosphate dehydrogenase (*GAPD*, NM_002046) was used to normalize the expression levels in the subsequent quantitative analyses. To amplify the target genes, the following primers were purchased from TaKaRa (Yotsukaichi, Japan): SRPX2-FW, ACT GGA TTT GCG GCA TGT GA; SRPX2-RW, CCA TGT TGA AGT AGG AGC GAG TGA; GAPD-FW, GCA CCG TCA AGG CTG AGA AC; GAPD-RW, ATG GTG GTG AAG ACG CCA GT.

Anti-SRPX2 polyclonal antibody

Rabbit antibodies specific for SRPX2 were obtained by immunizing rabbits with SRPX2 peptide (FIDDYLLSNQELTQ) according to a previously described method,[2] and IgG was purified from serum using standard protocols.

SRPX2-conditioned medium

The media in which subconfluent HEK293-pQCLIN-EGFP, HEK293-pQCLIN-SRPX2, MKN1-pQCLIN-EGFP and MKN1-pQCLIN-SRPX2 cells were being cultured was replaced with a serum-reduced medium (OPTI-MEM; GIBCO), the cells were cultured for an additional 24 hr and the conditioned-media were collected. The media were filtered using Millex-GS (Millipore, Bedford, MA) and concentrated using the Amicon Ultra (Millipore) and stored at −80°C. The concentration of the conditioned-medium was measured using a BCA protein assay (Pierce Biotechnology, Rockford, IL) and equalized.

Western blot analysis

The antibodies used in this study were anti-GFP (Invitrogen, Carlsbad, CA), anti-focal adhesion kinase (anti-FAK), anti-p-FAK (pY397) (BD Biosciences), anti-β-actin (Santa Cruz Biotechnology, Santa Cruz, CA) and anti-p-FAK (pY576/577) (Cell Signaling, Beverly, MA).

A Western blot analysis was performed as described previously (Ref. 10). In brief, subconfluent cells were washed with cold phosphate-buffered saline (PBS) and harvested with Lysis A buffer containing 1%Triton X-100, 20 mM Tris-HCl (pH 7.0), 5 mM EDTA, 50 mM sodium chloride, 10 mM sodium pyrophosphate, 50 mM sodium fluoride, 1 mM sodium orthovanadate and a protease inhibitor mix, complete™ (Roche Diagnostics). Whole-cell lysates and culture medium were separated using a 2–15% gradient SDS-PAGE and blotted onto a polyvinylidene fluoride membrane. After blocking with 3% bovine serum albumin in a TBS buffer (pH 8.0) with 0.1% Tween-20, the membrane was probed with primary antibody. After rinsing twice with TBS buffer, the membrane was incubated with horseradish peroxidase-conjugated secondary antibody (Cell Signaling) and washed followed by visualization using an ECL detection system (Amersham) and LAS-3000 (Fujifilm, Tokyo, Japan). The data were quantified by automated densitometry using Multigauge Ver 3.0 (Fujifilm).The experiment was performed in triplicate.

Cellular growth assay

HEK293 transfectant cells were incubated on 96-well plates at a density of 2000/well with 180 μL of culture medium at 37°C in 5% CO_2. After 24, 48 or 72 hr of incubation, 20 μL of MTT [3-(4,5-dimethyl-thiazoyl-2-yl)2,5-diphenyltetrazolium bromide] solution (SIGMA) was added and the cultures were incubated for 4 hr at 37°C. After centrifugation, the culture medium was discarded and the wells were filled with DMSO. The absorbance of the cultures at 562 nm was measured using VERSAmax (Japan Molecular Devices, Tokyo, Japan). The experiment was performed in triplicate.

Cellular adhesion assay

EGFP-conditioned or SRPX2-conditioned media obtained from HEK293-pQCLIN-EGFP, HEK293-pQCLIN-SRPX2, MKN1-pQCLIN-EGFP or MKN1-pQCLIN-SRPX2 cells were adjusted to a concentration of 1 mg/mL and 50 μL were incubated at 4°C overnight on 96-well plates. The conditioned media were aspirated, and the wells were washed twice with PBS. The plates were then used in an adhesion assay as conditioned medium-coated 96-well plates. The cells to be analyzed were added to the wells of conditioned medium-coated plates (2×10^4 cells /well) and incubated at 37°C for 1 hr. When treated with FAK inhibitors (PP2 and Herbimycin A; Calbiochem, San Diego, CA), the cells to be analyzed were incubated for 4 hr. The wells were then washed twice with PBS to remove nonadherent cells. Adherent cells were evaluated using the MTT assay as described above. The average O.D. values of 3 wells were used for a single experiment, and the experiment was performed in triplicate.

Migration assay and chemotaxis assay

Migration assays were performed using the Boyden-chamber methods and polycarbonate membranes with an 8-μm pore size

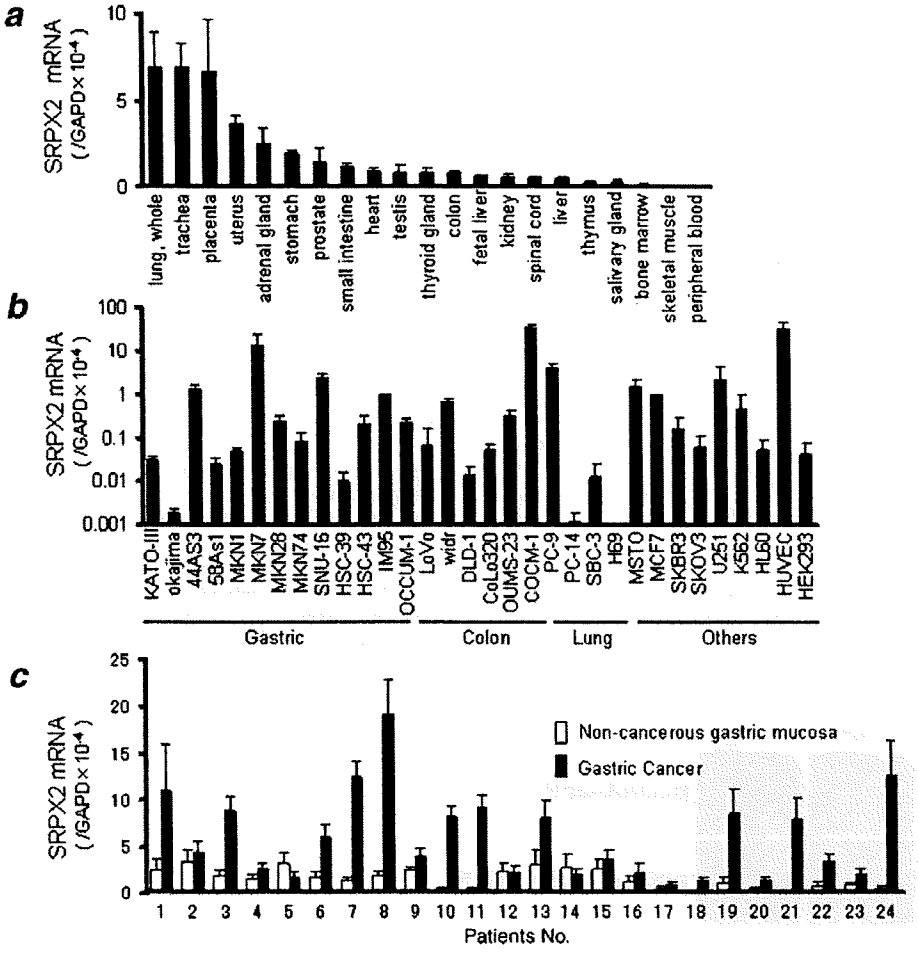

FIGURE 1 – Tissue distribution of *SRPX2* mRNA expression. The mRNA expression levels of *SRPX2* were determined using a real-time RT-PCR analysis in (*a*) human normal tissue; (*b*) 30 human cancer cell lines, HEK293 and HUVEC cell lines and (*c*) paired clinical samples that were endoscopically obtained from gastric cancer and the noncancerous gastric mucosa of the same patients. *GAPD* was used to normalize the expression levels in the subsequent quantitative analyses. The mRNA expression levels of *SRPX2* were significantly higher in the gastric cancer lesions ($p = 0.0004$). Error bars represent the SDs of 3 independent experiments. [Color figure can be viewed in the online issue, which is available at www.interscience.wiley.com.]

(chemotaxicell; KURABO). The membranes were coated with fibronectin on the outer side and dried for 2 hr at room temperature. The cells to be analyzed (2×10^4/well) were then seeded onto the upper chambers with 200 μL of migrating medium (DMEM containing 0.5% FBS), and the upper chambers were placed into the lower chambers of 24-well culture dishes containing 600 μL of DMEM containing 10% FBS. After incubation for 8 hr at 37°C, the media in the upper chambers were aspirated and the nonmigrated cells on the inner sides of the membranes were removed using a cotton swab. The cells that had migrated to the outer side of the membranes were fixed with 4% paraformaldehyde for 10 min and stained with 0.1% crystal violet for 15 min, then counted using a light microscope. The experiment was performed in triplicate.

The chemotaxis assays were performed using SNU-16 cells. A total of 1×10^5 cells were seeded onto the upper chambers with 200 μL of RPMI containing 0.5% FBS. The final concentration at 100 μg/mL of EGFP-conditioned or SRPX2-conditioned medium was added to the 600 μL volume of RPMI1640 containing 0.5% FBS medium in the lower chamber of the 24-well culture dishes. The cells were then incubated for 24 hr at 37°C with 5% CO_2. The number of migrated cells was evaluated as described earlier. The experiment was performed in triplicate.

Wound healing assay

HEK293-pQCLIN-EGFP and HEK293-pQCLIN-SRPX2 cells were plated onto 3.5-cm dishes and incubated in DMEM containing 10% FBS until they reached confluence. Wounds were introduced to the confluent cell monolayer using a plastic pipette tip. The cells were then cultured with DMEM containing 10% FBS at 37°C. After 4, 8 and 12 hr later, the wound area was photographed using a light microscope and measured. The experiment was performed in triplicate.

Fluorescent microscopy

HEK293-pcDNA-GFP and HEK293-pcDNA-SRPX2/GFP cells were treated with DAPI (6-diamidino-2-phenylindole) to stain the nucleus and photographed using fluorescent microscopy, IX71 (Olympus, Tokyo, Japan).

Statistics

The *t* test was used for comparison between 2 groups and paired *t* test was used for paired-samples in Figure 1*c*. The statistical analysis was performed using Excel software (Microsoft, Redmond, WA). A p value < 0.05 was considered significant.

Results

Tissue distribution of SRPX2 mRNA in normal tissues and cell lines

To examine the tissue distribution of *SRPX2* mRNA, we performed real-time RT-PCR for 24 normal human tissues. High expression levels of *SRPX2* mRNA were detected in the placenta, lung, trachea, uterus and adrenal gland, whereas the levels in the peripheral blood, brain and bone marrow were relatively low (Fig. 1*a*). Combined with data from previous reports,[1,2] *SRPX2* mRNA

appears to be widely observed in normal tissues, with particularly high levels detected in the placenta and lung.

SRPX2 expression was also examined in 30 human cancer cell lines, HUVEC and HEK293 cells. A relatively high *SRPX2* mRNA expression level was observed in gastric cancer (44As3, MKN7 and SNU-16), colorectal cancer (WiDr and COCM-1), lung cancer (PC-9), mesothelioma (MSTO), glioma (U251) and HUVEC. These results suggest that a variety of cancer and vascular endothelial cells express *SRPX2* (Fig. 1*b*).

TABLE I – *SRPX2* EXPRESSION AND PATIENT CHARACTERISTICS IN PATIENTS WITH GASTRIC CANCER

Characteristics	Patients No. (%)	*SRPX2* Expression (10^{-4}/*GAPD*)	*p* value
Age, years			
≥60	31 (54)	12.6 ± 12.5	0.10
<60	26 (46)	11.1 ± 9.1	
Sex			
Male	41 (72)	11.1 ± 9.1	0.61
Female	16 (28)	12.6 ± 12.5	
Histology[1]			
Diff.	22 (39)	11.3 ± 7.9	0.77
Undiff.	32 (56)	12.2 ± 11.7	
Prognosis[2]			
Favorable (≥6 months)	37 (65)	9.5 ± 7.2	<0.05
Unfavorable (<6 months)	20 (35)	15.1 ± 13.5	
Total	57		

[1]Histology of endoscopic samples divided into differentiated and undifferentiated type.–[2]Overall survival time from the first day of chemotherapy. A survival time of 6 months was used as the cut-off to divide patients into "Favorable" and "Unfavorable" groups.

Overexpression of SRPX2 mRNA in gastric cancer tissues

The expression of *SRPX2* mRNA was analyzed for paired tissues of gastric cancer and noncancerous gastric mucosa obtained from 24 gastric cancer patients. A paired *t* test demonstrated that *SRPX2* expression was significantly increased ($p = 0.0004$) in the cancerous tissues, compared to the noncancerous gastric mucosa (Fig. 1*c*). The *SRPX2* mRNA expression levels in the gastric cancer and noncancerous gastric mucosa were 6.6 ± 5.4 and 1.8 ± 1.2 ($\times 10^{-4}$/*GAPD*), respectively. Although the reason is unclear, 2 groups seemed to be present: 1 group with very high expression levels in cancerous tissues and another group with no difference in the expression levels between cancerous and noncancerous lesions.

To clarify the clinical significance of *SRPX2* expression, we examined the expression in an additional 57 gastric cancer samples using real-time RT-PCR and analyzed the correlations between *SRPX2* expression and clinical characteristics (Table I). Age, sex and histological cancer type were not correlated with *SRPX2* expression. However, patients with an unfavorable outcome, in whom the overall survival time (OS) was less than 6 months, exhibited significantly high expression levels of *SRPX2* in

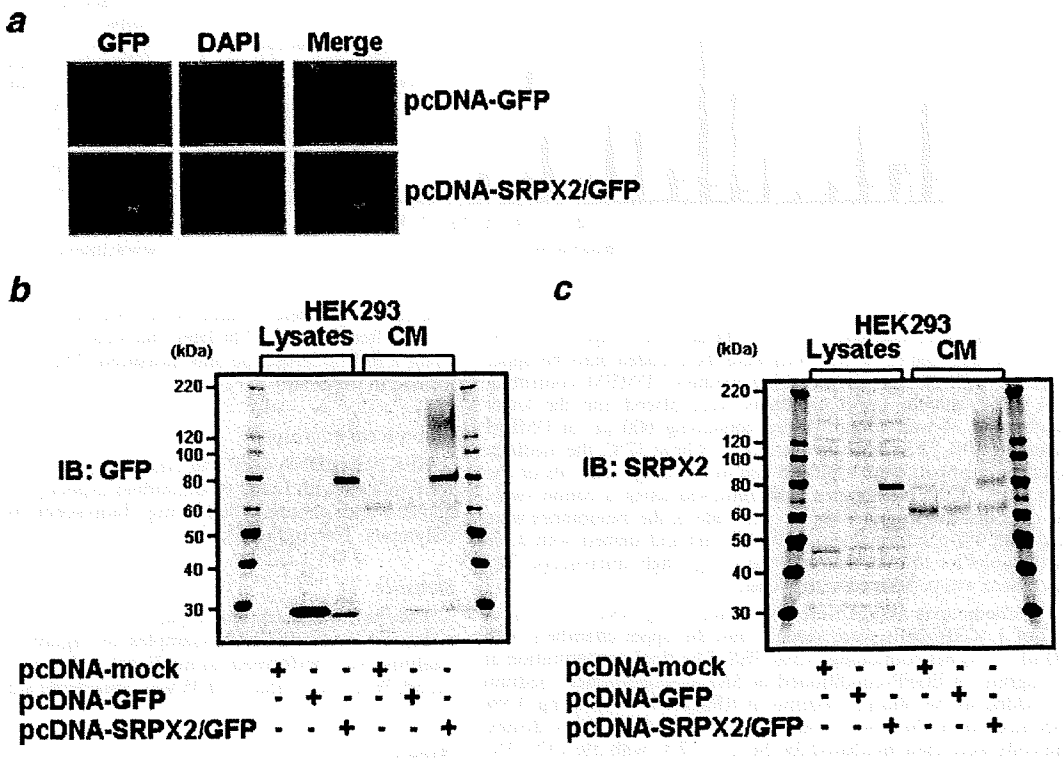

FIGURE 2 – Cellular distribution of SRPX2-GFP fusion protein. To examine the cellular distribution of SRPX2, we created cell lines expressing a fusion protein of SRPX2-GFP. The empty vector, GFP and SRPX2-GFP vectors were transfected into HEK293 cells using FuGENE6 transfection reagent. The vectors and stable transfectant cells in the HEK293 cells were designated as pcDNA-mock, pcDNA-GFP, pcDNA-SRPX2/GFP, HEK293-pcDNA-mock, HEK293-pcDNA-GFP and HEK293-pcDNA-SRPX2/GFP. (*a*) Fluorescence microscopy of HEK293-pcDNA-GFP (upper panel) and pcDNA-SRPX2/GFP cells (lower panel). The SRPX2/GFP fusion protein (green) showed a cytoplasmic distribution. The nucleus was stained by DAPI (blue). Western blot analysis detected by (*b*) anti-GFP antibody and (*c*) anti-SRPX2 antibody for HEK293-pcDNA-mock, HEK293-pcDNA-GFP and HEK293- pcDNA-SRPX2/GFP cells. Both the anti-GFP and the anti-SRPX2 antibodies detected the SRPX2-GFP fusion protein at ~80 kDa in the cell lysate and the secreted form at 150–180 kDa. IB, immunoblot; CM, culture medium.

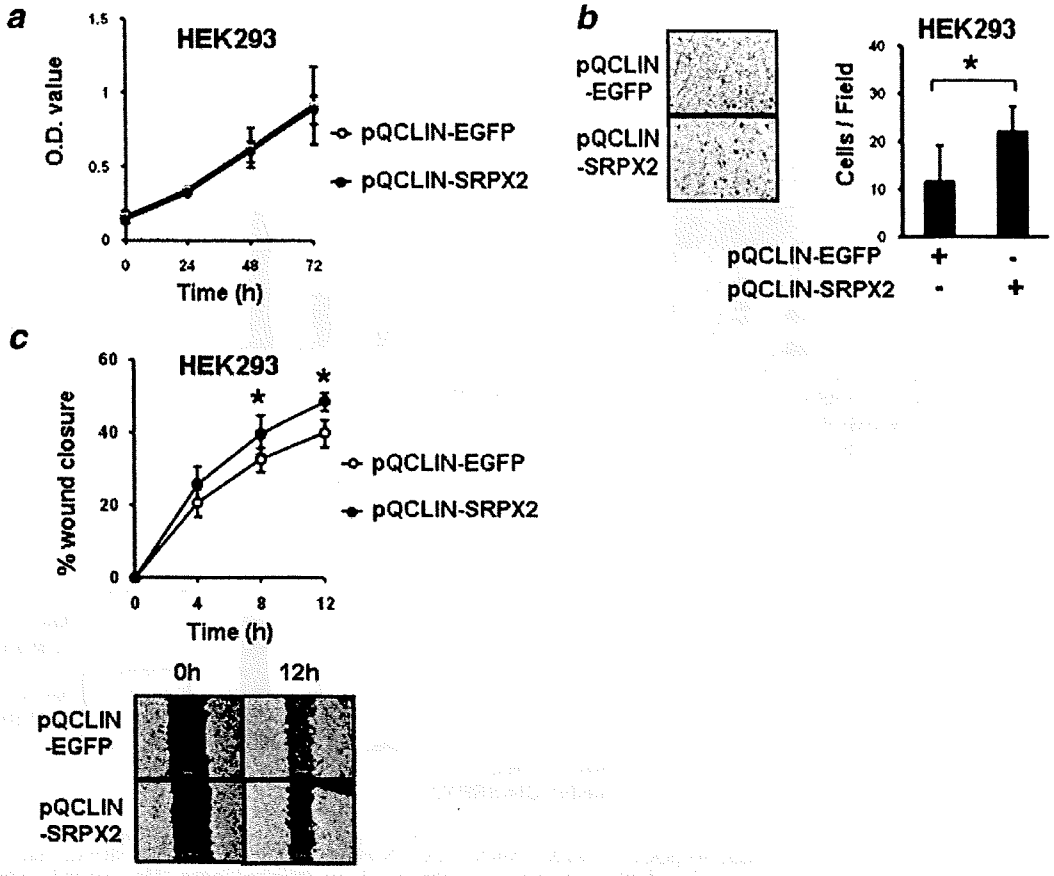

FIGURE 3 – SRPX2-introduced cells enhanced cellular migration but not cellular growth. Viral vectors containing EGFP and SRPX2 were constructed as pQCLIN-EGFP and pQLIN-SRPX2, respectively. These stable cell lines, retrovirally introduced into HEK293 cells, were designated as HEK293-pQCLIN-EGFP and HEK293-pQCLIN-SRPX2, respectively. (*a*) Cellular growth was examined using an MTT assay. No difference in cellular growth was observed between HEK293-pQCLIN-EGFP and HEK293-pQCLIN-SRPX2 cells. (*b*) Migration assay. Cells (2×10^4/well) were seeded into the upper chambers with serum-reduced medium (DMEM with 0.5% FBS). The upper chambers, with fibronectin coated on the outer side of the membrane, were then placed in the lower chambers of a 24-well culture plate containing DMEM with 10% FBS. After incubation for 8 hr at 37°C, medium was aspirated and the nonmigrated cells on the inner side of the membrane were removed using a cotton swab. The migrated cells on the outer side of the membrane were fixed, stained and counted using a light microscope. The experiment was performed in triplicate. The left panels show representative data. (*c*) Wound healing assay for HEK293-pQCLIN-EGFP and HEK293-pQCLIN-SRPX2 cells. Wounds were introduced to the confluent cell monolayer using a plastic pipette tip. After 4, 8 and 12 hr, the wound area was photographed and measured. The lower panels show representative data. The experiment was performed in triplicate. *: $p < 0.05$. EGFP, enhanced green fluorescent protein.

cancerous tissues ($p < 0.05$). The *SRPX2* expression levels in patients with an unfavorable outcome (OS < 6 months) and in those with a favorable outcome (OS > 6 months) were 9.5 ± 7.2 and 15.1 ± 13.5 ($\times 10^{-4}$/*GAPD*), respectively. This result suggests that *SRPX2* might be a prognostic biomarker, that is, associated with a malignant phenotype in gastric cancer.

SRPX2 is secreted into culture medium and localized in cytoplasm

Because the cellular distribution of an uncharacterized protein often suggest its biological function (*e.g.*, transcription factors tend to be localized in the nucleus), we tried to identify the cellular distribution of SRPX2 using a SRPX2-GFP fusion protein. We introduced an empty vector, GFP, or SRPX2 fused with GFP into HEK293 cells to create the following stable cell lines: HEK293-pcDNA-mock, HEK293-pcDNA-GFP and HEK293- pcDNA-SRPX2/GFP, respectively. The SRPX2-GFP fusion protein exhibited a cytoplasmic distribution (Fig. 2*a*). The protein expression of SRPX2 was then analyzed using western blotting and both anti-GFP and anti-SRPX2 antibodies (Figs. 2*b* and 2*c*). Western blotting with anti-GFP antibody revealed that an SRPX2-GFP fusion protein with a molecular weight (M.W.) of ~80 kDa was detected in both the cell lysates and the culture medium. A similar result was observed using anti-SRPX2 antibody. In addition, an SRPX2/GFP protein with a molecular weight of 150–180 kDa was observed in the culture medium when analyzed using both anti-GFP and anti-SRPX2 antibodies. The SRPX2 protein was detected as 2 bands with molecular weights of ~80 kDa and 150–180 kDa (containing a GFP protein of 30 kDa). The band was consistent with the estimated molecular weight of SRPX2, 53 kDa. The higher band was only observed in the culture medium and was detected using both anti-GFP and anti-SRPX2 antibodies.

SRPX2-introduced cells enhanced cellular migration but not cellular growth

To elucidate the biological function of SRPX2, EGFP or SRPX2 was retrovirally introduced into HEK293 cells. The stable cell lines were designated as HEK293-pQCLIN-EGFP and HEK293-pQCLIN-SRPX2, respectively. We then performed cellular growth assays using these cells (Fig. 3*a*). No difference in

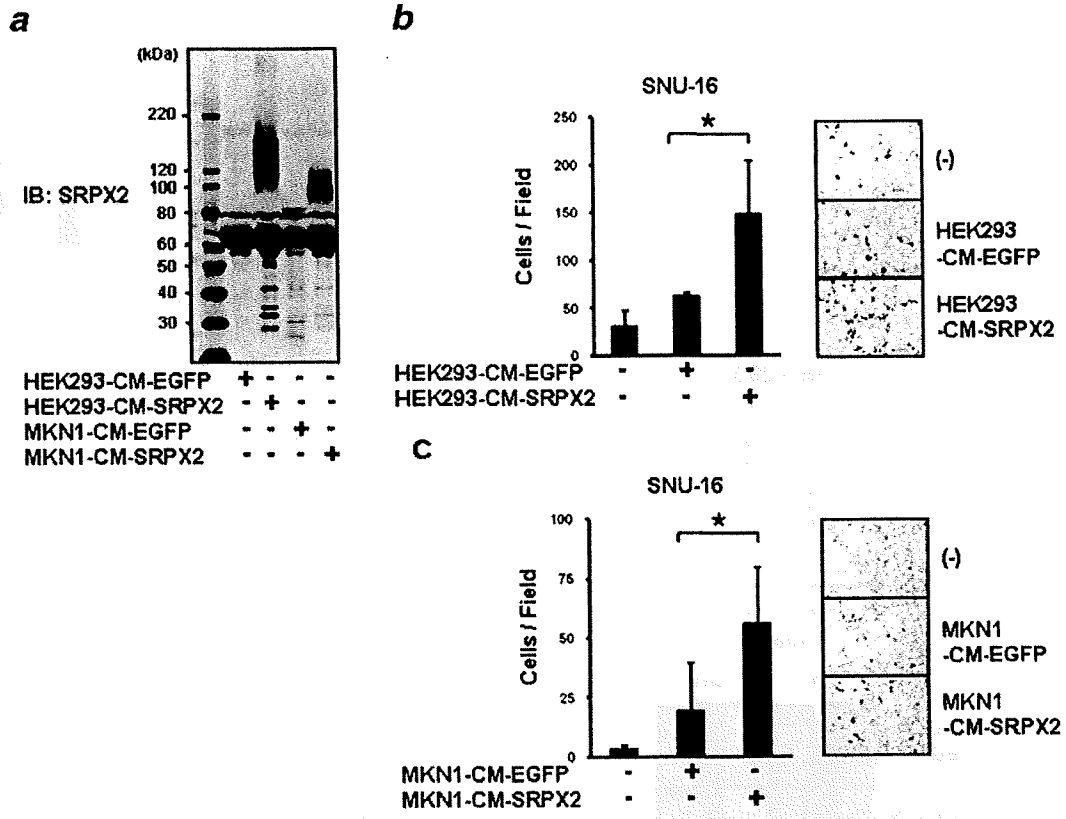

FIGURE 4 – SRPX2-conditioned medium enhanced cellular migration. (*a*) Western blotting for conditioned medium obtained from the stable cell lines, HEK293-pQCLIN-EGFP, HEK293-pQCLIN-SRPX2, MKN1-pQCLIN-EGFP and MKN1-pQCLIN-SRPX2. Each concentration of conditioned medium was adjusted to 1 mg/mL and diluted before use. Further details are described in the "Material and methods" section. IB, immunoblotting; HEK293-CM-EGFP, conditioned medium from HEK293-pQCLIN-EGFP cells; HEK293-CM-SRPX2, conditioned medium from HEK293-pQCLIN-SRPX2 cells; MKN1-CM-EGFP, conditioned medium from MKN1-pQCLIN-EGFP cells; MKN1-CM-SRPX2, conditioned medium from MKN1-pQCLIN-SRPX2 cells. The role of SRPX2 in cellular migration was assessed in the gastric cancer cell line, SNU-16, using a migration assay and EGFP- or SRPX2-conditioned medium from (*b*) HEK293-pQCLIN-EGFP or -SRPX2 cells and from (*c*) MKN1-pQCLIN-EGFP or -SRPX2 cells. A total of 1×10^5 SNU-16 cells were seeded into the upper chambers with 200 μL of RPMI containing 0.5% FBS. The final concentration of 100 μg/mL of EGFP-conditioned or SRPX2-conditioned medium was added to the 600 μL volume of the RPMI1640 containing 0.5% FBS medium in the lower chamber of the 24-well culture dish. The cells were incubated for 24 hr at 37°C. The number of migrated cells was evaluated as described earlier. The experiment was performed in triplicate. Representative data is shown in the right panels. The SRPX2-conditioned medium significantly enhanced cellular motility ($p < 0.05$) by about 2-fold, compared to the EGFP-conditioned medium. Data are shown as the mean ± SD of 3 independent experiments. *: $p < 0.05$.

cellular growth was seen between the cells, indicating that SRPX2 is not involved in cellular growth in HEK293 cells.

We next performed a migration assay to assess the role of SRPX2 in cellular motility. The cellular migration activity of the HEK293-pQCLIN-SRPX2 cells was significantly enhanced, compared to the EGFP transfectant cells ($p = 0.03$, Fig. 3*b*). A wound healing assay also demonstrated that the cellular motility of HEK293-pQCLIN-SRPX2 cells was significantly enhanced, compared to that of EGFP transfectant cells, at 8 and 12 hr after wound infliction ($p < 0.05$, Fig. 3*c*). Although the actual difference in the wound healing assay result was relatively small, these results indicate that SRPX2 is involved in cellular motility.

SRPX2-conditioned medium enhanced cellular migration

EGFP or SRPX2 was also introduced into a gastric cancer cell line, MKN1, and the SRPX2-conditioned media obtained from MKN1 and HEK293 cells were subjected to a migration assay. The transfected cells mainly produced the secreted type of SRPX2 protein with the higher molecular weight, as detected using western blot analysis. The SRPX2 proteins produced by MKN1 and HEK293 cells were observed at ~95 kDa and 110–150 kDa, respectively (Fig. 4*a*). This difference in molecular weight might be due to glycosylation.

The role of the secreted SRPX2 protein in the conditioned medium on cellular migration was assessed to SNU-16 cells using a migration assay. SNU-16 cells were incubated for 24 hr in a normal culture medium containing 100 μg/mL of EGFP- or SRPX2-conditioned medium from HEK293-pQCLIN-EGFP or -SRPX2 cells added to the lower chamber of the 24-well culture dish. The SRPX2-conditioned medium significantly enhanced the cellular motility of the SNU-16 cells ($p < 0.05$) by about 2-fold higher than that of the EGFP-conditioned medium (Fig. 4*b*). Similar results were observed using conditioned medium from MKN1-pQCLIN-EGFP or -SRPX2 cells (Fig. 4*c*). This result indicates that the secreted SRPX2 protein increased cellular motility in gastric cancer cells.

SRPX2 protein promoted cellular attachment

We examined the cellular adhesion potential of 7 gastric cancer cell lines cultured on EGFP- and SRPX2-conditioned medium-

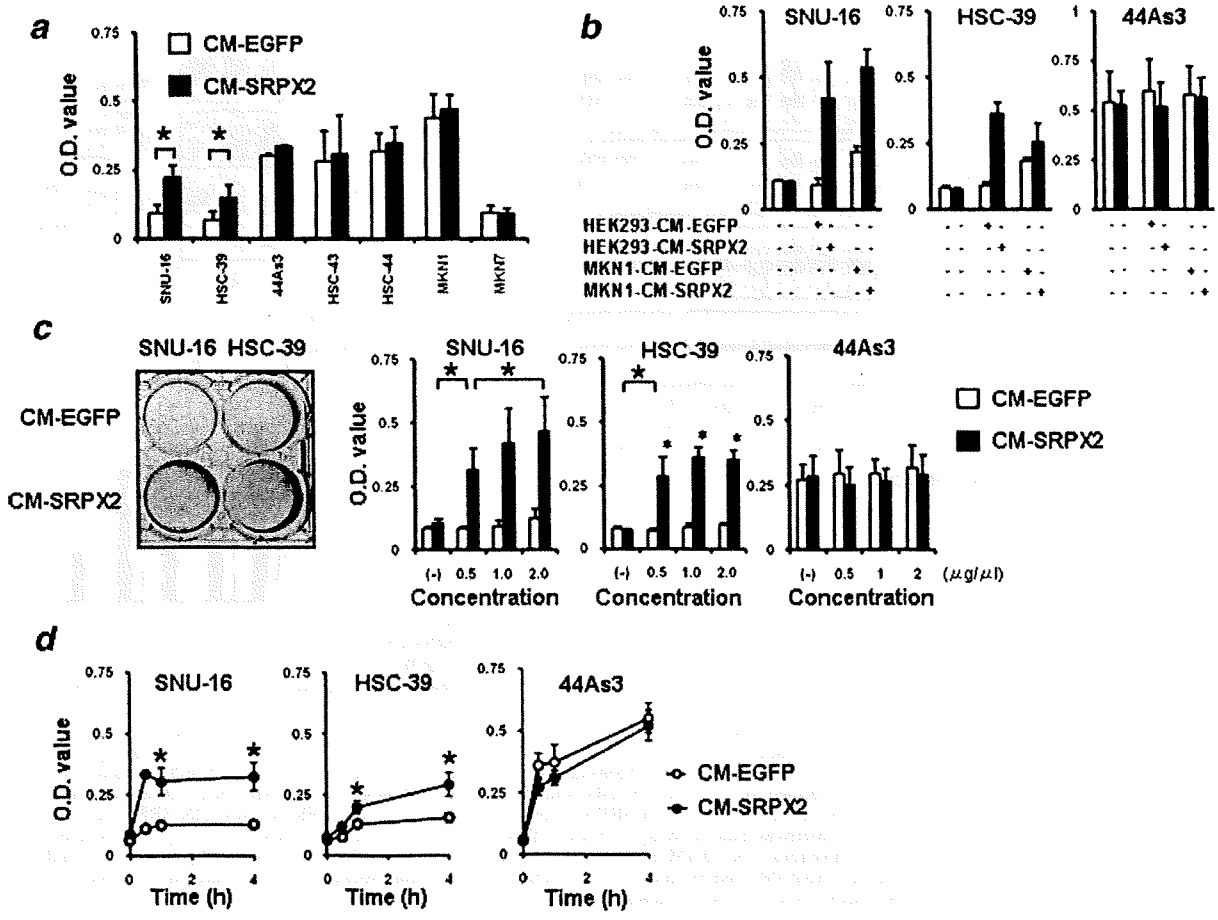

FIGURE 5 – SRPX2 protein enhanced cellular attachment. EGFP-conditioned or SRPX2-conditioned medium was adjusted to a concentration of 1 mg/mL and 50 μL was placed at 4°C overnight on 96-well plates. The conditioned medium was aspirated, and the wells were washed twice with phosphate-buffered saline (PBS). The plates were used in the adhesion assay as conditioned medium-coated 96-well plates. The cells to be analyzed (2×10^4 cells /well) were seeded into the wells of conditioned medium-coated plates and incubated at 37°C for 1 hr. The wells were then washed twice with PBS to remove nonadherent cells. The adherent cells were evaluated using an MTT assay. (*a*) A cellular adhesion assay was performed using 7 gastric cancer cell lines and conditioned medium-coated plates. The numbers of adhered SNU-16 and HSC-39 cells were significantly larger with the SRPX2-conditioned medium coated-plates ($p < 0.05$). (*b*) A cellular adhesion assay was also performed using conditioned medium-coated plates obtained from MKN1-pQCLIN-EGFP and MKN1-pQCLIN-SRPX2 cells. The numbers of adhered SNU-16 and HSC-39 cells, but not 44As3 cells, were significantly larger. (*c*) A cellular adhesion assay was performed using different concentrations of conditioned medium-coated plates. The 6-well-plate-scale data is shown in the left panel. (*d*) Cellular adhesion assay for time-course analysis. Larger numbers of attached SNU-16 and HSC-39 cells were observed from 0.5 to 4 hr. The increase in cellular attachment induced by the SRPX2 protein emerged after a relatively short time (0.5 hr). The experiment was performed in triplicate. CM-EGFP, conditioned medium from HEK293-pQCLIN-EGFP cells; CM-SRPX2, conditioned medium from HEK293-pQCLIN-SRPX2 cells. [Color figure can be viewed in the online issue, which is available at www.interscience.wiley.com.]

coated plates. Five of the gastric cancer cell lines did not increase cellular attachment to the conditioned medium-coated plate. However, the numbers of attached SNU-16 and HSC-39 cells were significantly increased by more than 2-fold by the presence of SRPX2 protein ($p < 0.05$, Fig. 5*a*).

To exclude nonspecific effects, cellular adhesion assays were also performed using conditioned medium-coated plates obtained from MKN1-pQCLIN-EGFP and MKN1-pQCLIN-SRPX2 cells (Fig. 5*b*). The SNU-16 and HSC-39 cells, but not the 44As3 cells, also exhibited a significantly larger number of adhered cells in the presence of SRPX2 protein obtained from the conditioned-medium of MKN1 cells. Cellular adhesion in these 3 cell lines was examined using 4 different concentrations of conditioned medium-coated plates. Similar results were obtained, and a dose-response effect for the conditioned medium was observed in SNU-16 cells (Fig. 5*c*). Time-course experiments revealed that a larger number of attached SNU-16 and HSC-39 cells were observed after a short time (0.5 hr) to 4 hr after the start of incubation (Fig. 5*d*). Microscopic examination revealed that most of the adhered cells did not exhibit "cell spreading" and instead resembled "cellular attachment." These results demonstrate that SRPX2 is involved in cellular attachment in SNU-16 and HSC-39 cells.

SRPX2 protein increased phosphorylation levels of FAK

FAK plays a key role in cellular adhesion, and FAK signaling is considered to be a major pathway.[11] To gain insight into the function of SRPX2, the phosphorylation levels of FAK in SNU-16 cells were examined after culturing in a medium to which SRPX2-conditioned medium had been added. Increased phosphorylation levels of FAK (pY397 and pY576/577) were observed in SNU-16 cells in the presence of SRPX2, compared to EGFP, after 1–12 hr of culture (Fig. 6*a*). FAK phosphorylation occurred during an early stage (1 hr) and was consistent with the results for cellular

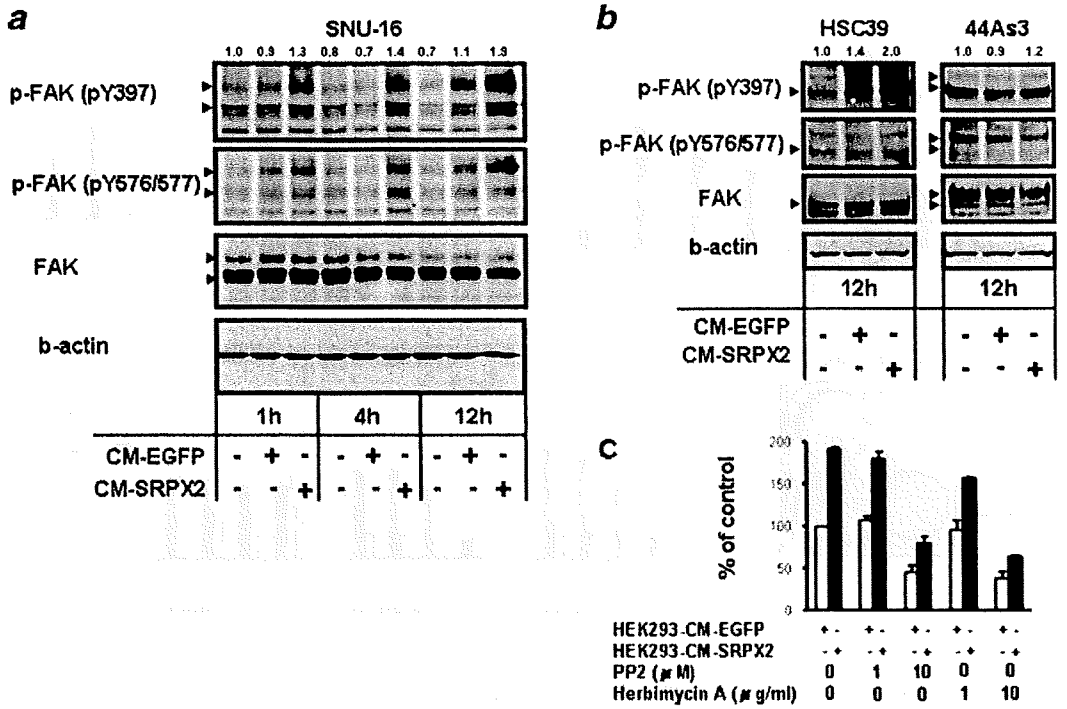

FIGURE 6 – SRPX2 protein increased the phosphorylation levels of FAK. The SNU-16 cells were cultured in RPMI with 0.5% FBS under the presence of GFP or SRPX2-conditioned medium at a final concentration of 100 μg /mL. The cells were collected at 1, 4 and 12 hr after incubation. Ten micrograms of cell lysate were subjected to western blotting using anti-phospho-FAK (pY397 and pY576/577), anti-FAK and anti-β-actin antibodies. A western blot was performed for (*a*) SNU-16 cells, and (*b*) HSC-39 and 44As3 cells. FAK, focal adhesion kinase; CM-EGFP, conditioned medium from HEK293-pQCLIN-EGFP cells; CM-SRPX2, conditioned medium from HEK293-pQCLIN-SRPX2 cells. Arrowheads: target molecules. The numerical densitometrical data of phospho-FAK (pY397) is shown above the western blot. (*c*) SNU-16 cells were treated with FAK inhibitors (PP2; final concentrations 1 or 10 μM and Herbimycin A; final concentrations 1 or 10 μg/mL) in a cellular adhesion assay to assess SRPX2-mediated attachment. Both PP2 and Herbimycin A inhibited cellular attachment of SNU-16 cells in dose-dependent manners. [Color figure can be viewed in the online issue, which is available at www.interscience.wiley.com.]

attachment. FAK phosphorylation by SRPX2 was also stimulated in HSC-39 cells but not in 44As3 cells (Fig. 6*b*). In addition, to determine whether FAK inhibitors could affect the SPRX2-mediated cellular attachment, the SNU-16 cells were treated with PP2[12] and Herbimycin A[13] to inhibit FAK activity in cellular adhesion assay (Fig. 6*c*). PP2 and Herbimycin A inhibited cellular attachment of SNU-16 cells in dose-dependent manners.

Although the molecules that transduce the extracellular SRPX2 signal into an intracellular signal remain unknown, these results suggest that the cellular phenotype caused by SRPX2 is associated with the FAK signaling pathway.

Discussion

Considering the structural features of *SRPX2*, the presence of both the sushi-repeat domain and the HYR domains predict an adhesive function.[4,8] We demonstrated that *SRPX2* enhanced cellular motility and cellular attachment, and these findings were consistent with the structural prediction.

The selectin family is the closest family to *SRPX2* and *SRPX*.[3] Selectins are known as cellular adhesion molecules and play key roles in the mediation of early neutrophil rolling on and adherence to endothelial cells.[14] Selectins recognize glycosylated proteins or lipids as their ligands, and this modification is necessary for their interaction.[15] The phylogenetical similarity between *SRPX2* and selectins suggests a similar biological function. SNU-16 and HSC-39 cells are basically nonadherent, and the increase in their cellular attachment was a relatively rapid response (0.5 hr). While number of attached cells increased significantly, the attachments were weak and the cells did not spread on the plates. Thus, the increased cellular attachment induced by SRPX2 seems to resemble neutrophil rolling.

Because the DGEA motif is a potential integrin-binding motif[16] and this motif exists in the first sushi domain of SRPX2, we hypothesized that this motif is a critical binding site for SRPX2's ability to enhance cellular migration and attachment. We examined the inhibitory effect of the DGEA peptide[16] on cell migration and attachment, but no inhibitory effect was observed (data not shown). This result suggests that the cell migration and attachment induced by SRPX2 might be independent of DGEA sequence-mediated signal transduction, or such a sequon does not function in SRPX2.

FAK is a major focal adhesion-associated protein that transmits signals downstream of integrins. FAK signals control important biological events, including cell migration, proliferation and survival, through downstream molecules like Rho, Rac, Rap1, CDC42 and PAK.[11,17,18] Our results demonstrated that SRPX2 protein increased the phosphorylation levels of FAK in SNU-16 and HSC-39 cells, but not in 44As3 cells (Figs. 6*a* and 6*b*), and enhanced the cellular adhesive potential in SNU-16 and HSC-39 cells but not in 5 other cell lines (Fig. 5*a*). We speculate that certain molecules overexpressed in SNU-16 and HSC-39 cells may localize on the cell surface and bind to SRPX2 protein, activating FAK signaling. Recently, Royer-Zemmour *et al.*[19] demonstrated the interaction of SRPX2 with uPAR (plasminogen activator, urokinase receptor) as well as with other partners such as cathepsin B. Because uPAR particularly plays an important and well-known role in various tumoral processes including cell proliferation, migration, invasion and adhesion, and because uPAR-associated

intracellular signaling may act through FAK. The SRPX2/uPAR interaction might provide a possible molecular explanation for the role of SRPX2 in cancer.

Regarding the higher fuzzy smeared-band observed in only the culture medium (Figs. 2*b*, 2*c* and 4*a*), the size of the bands differed considerably between HEK293 and MKN1 cells (110–150 kDa and ~95 kDa, respectively). These results suggest that the higher smeared bands are probably not dimmers, but they may represent a highly glycosylated protein modification. We tried to cut off the N-glycans using N-glycosidase F, but the 150-kDa smeared band did not disappear. We plan to perform additional experiments to clarify the cause of the smeared band in future studies, the results of which will undoubtedly be useful in predicting the function of SRPX2.

Many studies have indicated that selectins, the family most similar to SRPX and SRPX2 proteins, increase the interaction between tumor cells and endothelial cells, leading to tumor progression and metastasis.[20,21] Thus selectins are considered promalignancy factors.[20] Recent reports have shown that selectins positively promote angiogenesis.[22,23] Because HUVEC cells express high levels of *SRPX2* mRNA, the involvement of *SRPX2* in angiogenesis should be clarified.

In this study, we demonstrated that *SRPX2* is overexpressed in gastric cancer, compared to noncancerous gastric mucosa from the same patients, at the transcriptional level. A real-time RT-PCR analysis of 32 cell lines revealed that other cancer cells also express high levels of *SRPX2* mRNA. *SRPX2* was also overexpressed by more than 10-fold in clinical samples of colorectal cancers, compared to paired colonic mucosa (unpublished data). Thus, *SRPX2* overexpression in cancer tissue may not be restricted to gastric cancers. We plan to further examine *SRPX2* expression using immunohistochemistry in clinical samples of other cancers in the future.

Although the meaning of *SRPX2* overexpression in gastric cancer is unclear, a real-time RT-PCR analysis of clinical samples showed that *SRPX2* expression is associated with a poor prognosis in patients with gastric cancer. *SRPX2* was first identified as a downstream molecule of *E2F-HLF* in pro-B acute leukemia with t(17;19) (q23;p13) and has since been reported to contribute to malignant phenotypes.[1] *E2F-HLF*-positive leukemia is characterized by a poor outcome with bone invasion, hypercalcemia and intravascular coagulation.[24] The clinical features of leukemia and our results for gastric cancer suggest that the biological function of *SRPX2* is concerned with oncogenic activity. Further investigations of clinical outcome in relation to *SRPX2* expression are needed.

In conclusion, we found that *SRPX2* is overexpressed in gastric cancer and plays roles in cellular migration and adhesion in cancer cells. These results provide novel insight into the biological function of *SRPX2* in cancer cells.

Acknowledgements

This work was supported by funds for the Third-Term Comprehensive 10-Year Strategy for Cancer Control and the program for the promotion of Fundamental Studies in Health Sciences of the National Institute of Biomedical Innovation (NoBio) and the Japan Health Sciences Foundation. The following people have played very important roles in the conduct of this project. Miss Hiromi Orita, Dr. Hisanao Hamanaka, Dr. Ayumu Goto, Dr. Hisateru Yasui, Dr. Junichi Matsubara, Dr. Natsuko Okita, Dr. Takako Nakajima, Dr. Atsuo Takashima, Dr. Kei Muro, Dr. Takashi Ura, Miss Hideko Morita, Miss Mari Araake, Dr. Hisao Fukumoto, Dr. Tatsu Shimoyama, Dr. Naoki Hayama, Dr. Masayuki Takeda, Dr. Hideharu Kimura, Miss Kazuko Sakai, Dr. Terufumi Kato and Dr. Jun-ya Fukai.

References

1. Kurosawa H, Goi K, Inukai T, Inaba T, Chang KS, Shinjyo T, Rakestraw KM, Naeve CW, Look AT. Two candidate downstream target genes for E2A-HLF. Blood 1999;93:321–32.
2. Roll P, Rudolf G, Pereira S, Royer B, Scheffer IE, Massacrier A, Valenti MP, Roeckel-Trevisiol N, Jamali S, Beclin C, Seegmuller C, Metz-Lutz MN, et al. SRPX2 mutations in disorders of language cortex and cognition. Hum Mol Genet 2006;15:1195–207.
3. Royer B, Soares DC, Barlow PN, Bontrop RE, Roll P, Robaglia-Schlupp A, Blancher A, Levasseur A, Cau P, Pontarotti P, Szepetowski P. Molecular evolution of the human SRPX2 gene that causes brain disorders of the Rolandic and Sylvian speech areas. BMC Genet 2007;8:72.
4. O'Leary JM, Bromek K, Black GM, Uhrinova S, Schmitz C, Wang X, Krych M, Atkinson JP, Uhrin D, Barlow PN. Backbone dynamics of complement control protein (CCP) modules reveals mobility in binding surfaces. Protein Sci 2004;13:1238–50.
5. Soares DC, Gerloff DL, Syme NR, Coulson AF, Parkinson J, Barlow PN. Large-scale modelling as a route to multiple surface comparisons of the CCP module family. Protein Eng Des Sel 2005;18:379–88.
6. Meindl A, Carvalho MR, Herrmann K, Lorenz B, Achatz H, Apfelstedt-Sylla E, Wittwer B, Ross M, Meitinger T. A gene (SRPX) encoding a sushi-repeat-containing protein is deleted in patients with X-linked retinitis pigmentosa. Hum Mol Genet 1995;4:2339–46.
7. Dry KL, Aldred MA, Edgar AJ, Brown J, Manson FD, Ho MF, Prosser J, Hardwick LJ, Lennon AA, Thomson K, Keuren MV, Kurnit DM, et al. Identification of a novel gene, ETX1 from Xp21.1, a candidate gene for X-linked retintis pigmentosa (RP3). Hum Mol Genet 1995;4:2347–53.
8. Callebaut I, Gilges D, Vigon I, Mornon JP. HYR, an extracellular module involved in cellular adhesion and related to the immunoglobulin-like fold. Protein Sci 2000;9:1382–90.
9. Yamada Y, Arao T, Gotoda T, Taniguchi H, Oda I, Shirao K, Shimada Y, Hamaguchi T, Kato K, Hamano T, Koizumi F, Tamura T, et al. Identification of prognostic biomarkers in gastric cancer using endoscopic biopsy samples. Cancer Sci 2008;99:2193–99.
10. Yamanaka R, Arao T, Yajima N, Tsuchiya N, Homma J, Tanaka R, Sano M, Oide A, Sekijima M, Nishio K. Identification of expressed genes characterizing long-term survival in malignant glioma patients. Oncogene 2006;25:5994–6002.
11. Parsons JT. Focal adhesion kinase: the first ten years. J Cell Sci 2003; 116:1409–16.
12. Pala D, Kapoor M, Woods A, Kennedy L, Liu S, Chen S, Bursell L, Lyons KM, Carter DE, Beier F, Leask A. Focal adhesion kinase/Src suppresses early chondrogenesis: central role of CCN2. J Biol Chem 2008;283:9239–47.
13. Lan CC, Wu CS, Chiou MH, Hsieh PC, Yu HS. Low-energy helium-neon laser induces locomotion of the immature melanoblasts and promotes melanogenesis of the more differentiated melanoblasts: recapitulation of vitiligo repigmentation in vitro. J Invest Dermatol 2006; 126:2119–26.
14. Mousa SA. Cell adhesion molecules: potential therapeutic & diagnostic implications. Mol Biotechnol 2008;38:33–40.
15. Vestweber D, Blanks JE. Mechanisms that regulate the function of the selectins and their ligands. Physiol Rev 1999;79:181–213.
16. Mineur P, Guignandon A, Lambert ChA, Amblard M, Lapiere ChM, Nusgens BV. RGDS and DGEA-induced [Ca2+]i signalling in human dermal fibroblasts. Biochim Biophys Acta 2005;1746:28–37.
17. Schaller MD. FAK and paxillin: regulators of N-cadherin adhesion and inhibitors of cell migration? J Cell Biol 2004;166:157–9.
18. Mitra SK, Schlaepfer DD. Integrin-regulated FAK-Src signaling in normal and cancer cells. Curr Opin Cell Biol 2006;18:516–23.
19. Royer-Zemmour B, Ponsole-Lenfant M, Gara H, Roll P, Leveque C, Massacrier A, Ferracci G, Cillario J, Robaglia-Schlupp A, Vincentelli R, Cau P, Szepetowski P. Epileptic and developmental disorders of the speech cortex: ligand/receptor interaction of wild-type and mutant SRPX2 with the plasminogen activator receptor uPAR. Hum Mol Genet 2008;17:3617–30.
20. Witz IP. The selectin-selectin ligand axis in tumor progression. Cancer Metastasis Rev 2008;27:19–30.
21. Barthel SR, Gavino JD, Descheny L, Dimitroff CJ. Targeting selectins and selectin ligands in inflammation and cancer. Expert Opin Ther Targets 2007;11:1473–91.
22. Oh IY, Yoon CH, Hur J, Kim JH, Kim TY, Lee CS, Park KW, Chae IH, Oh BH, Park YB, Kim HS. Involvement of E-selectin in recruitment of endothelial progenitor cells and angiogenesis in ischemic muscle. Blood 2007;110:3891–9.
23. Egami K, Murohara T, Aoki M, Matsuishi T. Ischemia-induced angiogenesis: role of inflammatory response mediated by P-selectin. J Leukoc Biol 2006;79:971–6.
24. Hunger SP. Chromosomal translocations involving the E2A gene in acute lymphoblastic leukemia: clinical features and molecular pathogenesis. Blood 1996;87:1211–24.